Nigerian Journal of Physics (NJP)
ISSN online: 3027-0936
ISSN print: 1595-0611
DOI: https://doi.org/10.62292/njp.v35i4.2026.689
Volume 35(4), December 2026

Geophysical and Physicochemical Investigation of Leachate Plume Distribution and Its Impact on Groundwater Resources in Some Parts of Nasarawa State

***[1]Paul Amade Emmanuel, [2]Adeeko Tajudeen Olugbenga and [3]Farouq Ado Umar**

[1]Department of Physics, Bingham University, Karu, Nasarawa State
[2]Department of Physics, University of Abuja, Nigeria
[3]Industrial Safety & Environmental Technology Department, Petroleum Training Institute Effurun, Delta State Nigeria

*Corresponding Author's Email: paulemmanuel@binghamuni.edu.ng Phone: +2348069619656

Keywords:
Groundwater contamination,
Leachate plume,
Electrical resistivity,
VES,
Physicochemical analysis,
Dumpsites,
Nasarawa State.

ABSTRACT

Groundwater contamination resulting from indiscriminate waste disposal has become a major environmental and public health concern in many developing countries, especially where groundwater serves as the primary source of domestic water supply. This study assessed the impact of leachate migration from selected dumpsites in Nasarawa State, Nigeria, on groundwater quality and subsurface conditions using an integrated geophysical and physicochemical approach. The research focused on delineating leachate plumes, evaluating groundwater contamination, and examining the hydrogeological implications of dumpsite activities. The methodology combined reconnaissance surveys, electrical resistivity investigations, and laboratory analysis of groundwater samples. Geophysical surveys involved Vertical Electrical Sounding (VES) using the Schlumberger array and two-dimensional (2D) resistivity imaging. Ten VES stations were established across Nasarawa Toto, Lafia Site 1, and Lafia Site 2, including control locations situated away from the dumpsites. Groundwater samples collected from boreholes were analyzed for physicochemical properties and heavy metal concentrations. The geophysical results revealed extensive low-resistivity anomalies associated with leachate-contaminated zones in the shallow subsurface. Resistivity values within contaminated topsoil and sandy clay layers ranged from 3.7 to 52.7 Ωm, whereas control locations recorded higher values between 52.3 and 123.9 Ωm, indicating relatively uncontaminated conditions. The contamination was mainly restricted to depths of 0–18.1 m, with evidence of lateral migration through permeable sandy clay formations. Lafia Site 2 exhibited the highest level of contamination, characterized by an extremely low resistivity value of 3.7 Ωm, while Lafia Site 1 showed deeper contaminant penetration due to highly permeable subsurface materials. The presence of fresh basement rocks with resistivity values exceeding 1000 Ωm acted as barriers to deeper contaminant movement. Water quality analysis confirmed significant groundwater deterioration near the dumpsites. Elevated concentrations of heavy metals, including cadmium, lead, nickel, cobalt, manganese, chromium, and copper, exceeded World Health Organization (WHO) permissible limits in several locations. High levels of nitrate, chloride, phosphate, sodium, conductivity, and turbidity further indicated strong leachate influence. The study concluded that uncontrolled dumpsite activities have adversely affected groundwater quality and altered subsurface geoelectrical properties, emphasizing the need for effective waste management practices, continuous groundwater monitoring, and remediation measures to safeguard public health and groundwater resources in Nasarawa State.

Submitted: 25 May 2026

Accepted: 15 Jun. 2026

Published: 05 Aug. 2026

INTRODUCTION

Groundwater constitutes a vital component of the global freshwater system and serves as a major source of potable water, particularly in regions undergoing rapid urbanization, demographic expansion, and increasing water demand. Notwithstanding its strategic importance to socioeconomic development and ecosystem sustainability, groundwater resources are increasingly subjected to intense anthropogenic pressure arising from excessive abstraction and the growing impacts of climatic variability (Lall, Josset, & Russo, 2020). Recent studies have shown that more than 20% of aquifer systems worldwide are currently overexploited, especially within arid and semi-arid environments where groundwater withdrawal rates substantially exceed natural recharge processes (Esteban, Calvo, & Albiac, 2021). Such persistent imbalance has resulted in significant hydrogeological and environmental consequences, including land subsidence, reduction in streamflow, and irreversible degradation of sensitive fluvial ecosystems (Jasechko et al., 2024; Pokhrel, Hanasaki, Wada, & Kim, 2016). In addition, the extensive dependence on groundwater for agricultural irrigation and industrial activities has intensified concerns regarding seawater intrusion, declining groundwater storage, and long-term aquifer exhaustion (Kuang et al., 2024; Loáiciga & Doh, 2023). Although more than 30% of the world's major aquifer systems are presently categorized as stressed, inadequate information on groundwater storage dynamics continues to hinder the development and implementation of sustainable groundwater management frameworks (Boretti & Rosa, 2019).

The susceptibility of groundwater systems to contamination is largely controlled by their hydraulic connectivity with surface processes and by the physicochemical characteristics of both the saturated and unsaturated subsurface zones (Hasan et al., 2019). Among the most critical sources of groundwater pollution is the infiltration of leachates derived from municipal landfills and open dumpsites, a phenomenon extensively documented in environmental and hydrogeophysical investigations (Ganiyu et al., 2015). In many developing countries, including Nigeria, indiscriminate solid waste disposal practices remain prevalent, with refuse frequently deposited in uncontrolled environments such as abandoned excavations, natural depressions, drainage pathways, and urban open spaces. These unsanitary disposal practices significantly enhance the potential for leachate migration into subsurface formations, thereby posing serious threats to groundwater quality and public health.

Furthermore, many of these sites are situated in proximity to residential zones and sensitive groundwater recharge areas, exacerbating the exposure pathways for local populations (Afolagboye, Ojo, & Talabi, 2020). In these regions, the absence of appropriate containment barriers allows toxic pollutants to penetrate the subsurface, leading to the bioaccumulation of heavy metals and the proliferation of pathogenic microorganisms within the surrounding ecosystems (Ahmad et al., 2021; Boateng, Opoku, & Akoto, 2019; Siddiqua, Hahladakis, & Al-Attiya, 2022). Beyond these immediate ecological concerns, the prevalence of open dumping and the lack of engineered leachate collection systems contribute to the pervasive contamination of surface water bodies, particularly when disposal sites are positioned in coastal proximity (Gunarathne et al., 2023).

In Nigeria, the prevalence of open waste disposal practices has largely been attributed to inadequate technological capacity, financial limitations, and insufficient public awareness regarding the associated environmental implications (Adewole, 2009; Ako et al., 1990). Consequently, the resulting leachate plumes migrate through porous soil layers, severely compromising the integrity of vital groundwater resources upon which many urban and peri-urban communities rely (Ariyo, Adegoke, Bayewu, Ishola, & Alaka, 2024; Ozoko, Onyekwelu, & Aghamelu, 2022). Beyond these direct health hazards, the lack of rigorous post-closure monitoring and regulatory enforcement further complicates remediation efforts for these contaminated aquifers (Anjali, Singh, Agarwal, Singh, & Gangwar, 2026). This situation is compounded by factors such as high soil permeability and shallow water tables, which accelerate the transport of dissolved solids and pathogens into drinking water supplies (Anjali, Singh, Agarwal, Singh, & Gangwar, 2026; Gutberlet & Uddin, 2017). This study aimed at using geophysical and physicochemical methods to identify and map leachate plume movement, assess groundwater contamination levels, and evaluate the impact of dumpsite activities on groundwater resources in Nasarawa State.

Geology of the Area

Nasarawa State is situated within the Middle Belt region of Nigeria, lying approximately between latitudes 7°45′–9°25′N and longitudes 7°–9°37′E, and encompassing a total land area of about 26,875.59 km² with an estimated population of 1.83 million based on the 2006 census. Geologically, the state forms part of the North-Central Nigerian Basement Complex and is predominantly characterized by the Younger Granite suite. Its lithological framework is generally grouped into three major assemblages: the undifferentiated migmatite complex of Archean to Proterozoic age, metavolcano-sedimentary sequences of Late Proterozoic origin, and the Older Granite Complex (Pan-African granites) of Late Precambrian to Lower Paleozoic age. These lithological units have undergone extensive deformation and reworking associated with the Pan-African thermotectonic event, which has played a key role in shaping their structural evolution and geochemical attributes (Oyawoye, 1972; Black et al., 1979; Ajibade et al., 1987).

The geology of Nassarawa state favours infiltrations of mineral-rich fluids along structural discontinuities, facilitating the concentration of diverse metallic and non-metallic deposits such as iron ore, lead-zinc, and barite (Okwesili, Yakubu, & Ossai, 2024). Dumpsites near sources of groundwater pose significant risks to water quality, as anthropogenic pollutants infiltrate the subsurface, potentially exacerbating the geogenic presence of heavy metals like lead and manganese (Akaamaa *et al.,* 2023). Furthermore, the state's diverse mineral wealth—including tantalite, cassiterite, and columbite—has spurred extensive mining activities that frequently alter the local hydrogeological landscape and increase the vulnerability of surrounding water bodies to toxic leachates (Akinlalu, Olowe, Afolabi, & Aladejana, 2025).

MATERIALS AND METHODS

The study employs a multidisciplinary methodological framework that integrates reconnaissance survey, geophysical investigation, and geochemical analysis to evaluate groundwater contamination within Karu Local Government Area, Nasarawa State. A preliminary field reconnaissance is undertaken to characterize the study environment through systematic mapping using a compass/clinometer, measuring tape, and GPS (Garmin GPS Map 7.8), complemented by direct field observations aimed at identifying key hydrogeological features and existing borehole locations.

The geophysical component is based on electrical resistivity techniques, with emphasis on two-dimensional (2D) resistivity imaging using the multiple-gradient array, alongside vertical electrical sounding (VES) employing the Schlumberger configuration. These methods are applied to delineate subsurface lithological variations, groundwater occurrence zones, and potential contaminant (leachate) migration pathways. Data acquisition is conducted using an ABEM Terrameter (SAS 1000/4000) equipped with electrodes, connecting cables, clips, and a stable power supply to ensure reliable measurement of subsurface resistivity variations. Three locations were identified for this research (Figure 1).

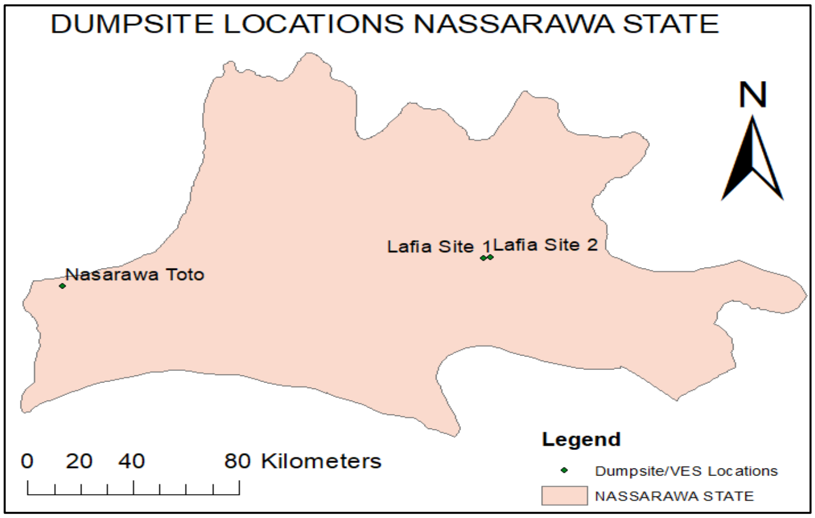

Figure 1: Dumpsite/VES Locations

Groundwater samples are systematically collected from boreholes aligned along dumpsites for laboratory-based physicochemical analysis. The Heavy Metal Pollution Index (HPI) is subsequently applied to quantify the degree of contamination. Finally, both geophysical and geochemical datasets are integrated to provide a comprehensive assessment of groundwater quality and contaminant distribution within the study area.

RESULTS AND DISCUSSION

The study involved the acquisition of Vertical Electrical Sounding (VES) data across seven selected locations within the study area to characterize subsurface conditions and evaluate possible contamination associated with dumpsite activities. The investigated sites include Nasarawa Toto (7°04′41.02″E, 8°23′21.11″N), Lafia Site 1 (8°30′56.55″E, 8°30′18.93″N), and Lafia Site 2 (8°32′8.25″E, 8°30′36.39″N). In total, ten VES stations were established across the study locations.

At each of the three principal areas, four VES measurements were carried out. Three of these were strategically sited in proximity to the dumpsites to capture subsurface variations potentially influenced by waste disposal activities, while one additional sounding point was positioned at a comparatively distant, unaffected location to serve as a control baseline for comparative analysis of geoelectrical responses.

Nasarawa Toto

The WinResist curve for Nasarawa Toto dumpsite VES 1, shown in Figure 2, exhibits an AA-type curve with four layers and increasing resistivity: 18.1 Ωm (0–1.8 m), 25 Ωm (1.8–8.2 m), 924.3 Ωm (8.2–26.7 m), and 3926.8 Ωm (26.7–40 m). The curves for VES 2, VES 3, and control point VES 4 are in the appendix. Dumpsite VES 2 and VES 3 also show AA-type curves with similar trends: 11.3–14.2 Ωm (0–1.2 m), 23.7–26.3 Ωm (0.8–8.4 m), and 1055.9–3638.9 Ωm (6.7–40 m). The control point VES 4 (HA-type) has higher resistivity: 106 Ωm (0–1.2 m), 52.3 Ωm (1.2–6.7 m), and 1588.5–8691.4 Ωm (6.7–40 m). The low resistivity in the upper layers of dumpsite curves suggests anomalies, while the control point's higher resistivity indicates a more resistive subsurface.

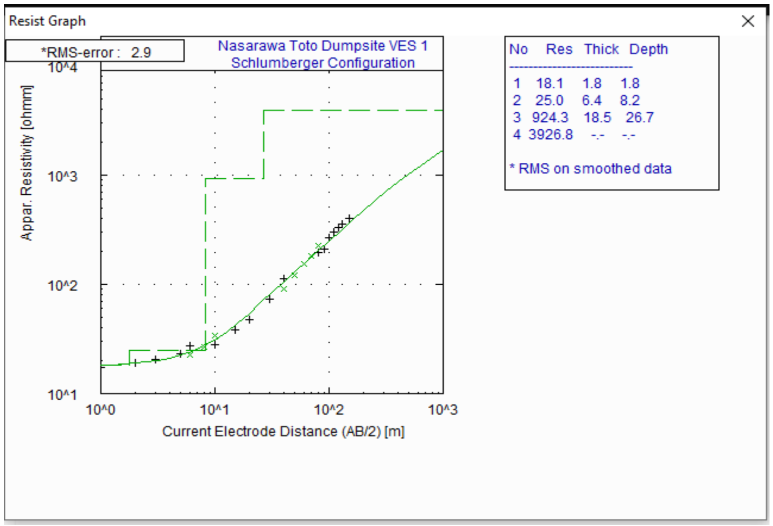

Figure 2: VES at Nasarawa Toto Dumpsite AA Curve-Type

Lafia Site 1

The WinResist curve for Lafia Site 1 dumpsite VES 1, presented in Figure 3, shows an AA-type curve with four layers and increasing resistivity: 13.1 Ωm (0–2 m), 175.1 Ωm (2–13.1 m), 492.6 Ωm (13.1–40.4 m), and 971.9 Ωm (40.4–50 m). The curves for VES 2, VES 3, and control point VES 4 are in the appendix. Dumpsite VES 2 (HA-type) has four layers: 25.6 Ωm (0–0.4 m), 7 Ωm (0.4–1.6 m), 204 Ωm (1.6–6.6 m), and 584.8 Ωm (6.6–50 m). VES 3 (AA-type) shows 21.6 Ωm (0–2.9 m), 175.5 Ωm (2.9–18.1 m), 491.1 Ωm (18.1–45.4 m), and 967 Ωm (45.4–50 m). The control point VES 4 (AA-type) has higher resistivity: 72.5 Ωm (0–3.3 m), 135.7 Ωm (3.3–15.2 m), 476 Ωm (15.2–54.8 m), and 869.4 Ωm (54.8–60 m). The low resistivity in VES 2's second layer (7 Ωm) indicates a significant anomaly.

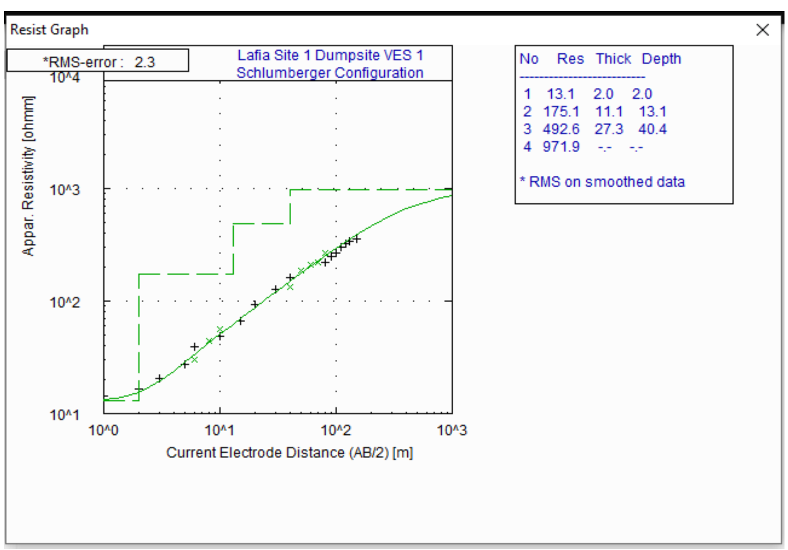

Figure 3: VES at Lafia Site 1 Dumpsite AA curve-type

Lafia Site 2

The WinResist curve for Lafia Site 2 dumpsite VES 1, shown in Figure 4, displays an HA-type curve with four layers: 18.2 Ωm (0–0.7 m), 3.7 Ωm (0.7–1.6 m), 3706.5 Ωm (1.6–54.3 m), and 2933.3 Ωm (54.3–60 m). The curves for VES 2, VES 3, and control point VES 4 are in the appendix. Dumpsite VES 2 and VES 3 (AA-type) show increasing resistivity: 31.3–52.3 Ωm (0–3.3 m), 36.1–52.7 Ωm (2.9–8.2 m), 552.2–635.8 Ωm (6.5–52.6 m), and 1303–1496.9 Ωm (41.6–60 m). The control point VES 4 (HA-type) has higher resistivity: 123.9 Ωm (0–0.6 m), 112.6 Ωm (0.6–10.9 m), 472.1 Ωm (10.9–56.8 m), and 1151.9 Ωm (56.8–60 m). The extremely low resistivity in VES 1's second layer (3.7 Ωm) suggests a significant anomaly.

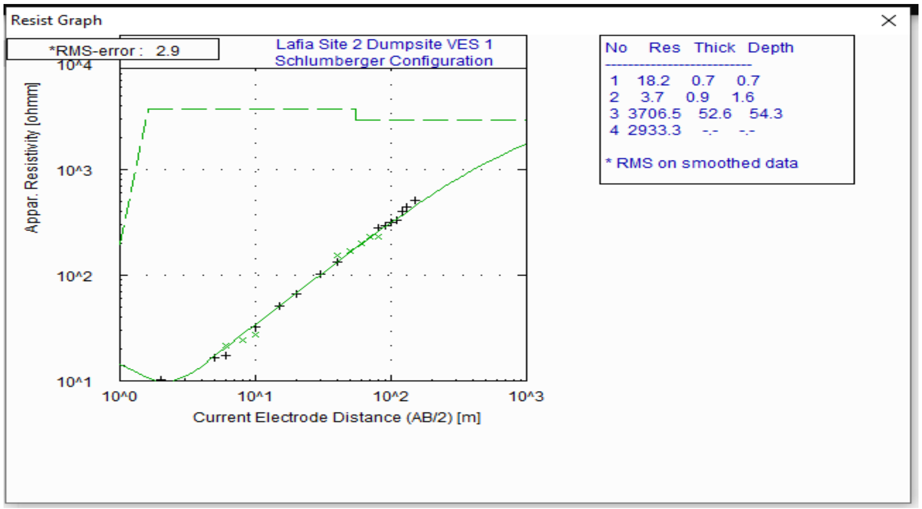

Figure 4: VES at Lafia Site 2 Dumpsite HA curve-type

Interpretations

Nasarawa Toto

The geoelectric log for Nasarawa Toto dumpsite VES 1, presented in Figure 5, shows four layers with inferred lithology, emphasizing thickness and depth ranges: Layer 1 (depth 0–1.8 m, thickness 1.8 m, 18.1 Ωm, topsoil), Layer 2 (depth 1.8–8.2 m, thickness 6.4 m, 25 Ωm, sandy clay), Layer 3 (depth 8.2–26.7 m, thickness 18.5 m, 924.3 Ωm, fresh basement), and Layer 4 (depth 26.7–40 m, thickness 13.3 m, 3926.8 Ωm, fresh basement). Logs for VES 2, VES 3, and control point VES 4 are in the appendix. Dumpsite VES 2 and VES 3 have three layers: VES 2 with Layer 1 (depth 0–0.8 m, thickness 0.8 m, 11.3 Ωm, topsoil), Layer 2 (depth 0.8–8.4 m, thickness 7.6 m, 26.3 Ωm, sandy clay), and Layer 3 (depth 8.4–40 m, thickness 31.6 m, 3750.2 Ωm, fresh basement); VES 3 with Layer 1 (depth 0–1.2 m, thickness 1.2 m, 14.2 Ωm, topsoil), Layer 2 (depth 1.2–6.7 m, thickness 5.5 m, 23.7 Ωm, sandy clay), and Layer 3 (depth 6.7–40 m, thickness 33.3 m, 3638.9 Ωm, fresh basement). The control point VES 4 has three layers: Layer 1 (depth 0–1.2 m, thickness 1.2 m, 106 Ωm, topsoil), Layer 2 (depth 1.2–6.7 m, thickness 5.5 m, 52.3 Ωm, clay), and Layer 3 (depth 6.7–40 m, thickness 33.3 m, 8691.4 Ωm, fresh basement). Dumpsite VES points have thinner or comparable upper layers (thickness 0.8–1.8 m vs. 1.2 m for topsoil; 5.5–7.6 m vs. 5.5 m for sandy clay/clay) with lower resistivity (11.3–18.1 Ωm vs. 106 Ωm in topsoil; 23.7–26.3 Ωm vs. 52.3 Ωm in sandy clay/clay), indicating potential pollution, while deeper layers have similar thickness and high resistivity.

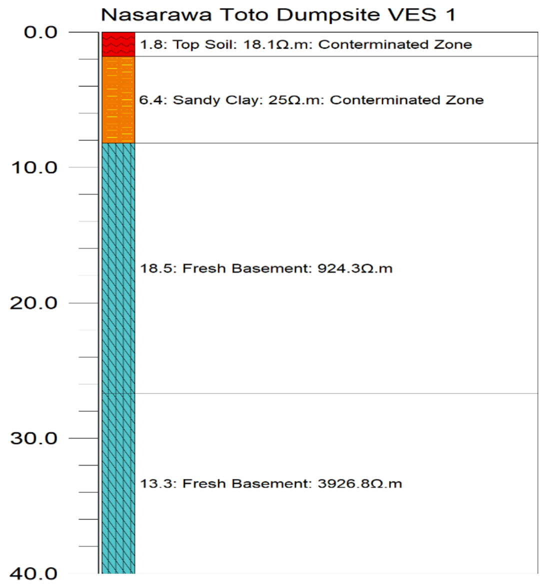

Figure 5: Geoelectric log for Nasarawa Toto dumpsite VES 1

This VES depicted four layers: topsoil (0–1.8 m, 18.1 Ωm), sandy clay (1.8–8.2 m, 25 Ωm), fresh basement (8.2–26.7 m, 924.3 Ωm), and fresh basement (26.7–40 m, 3926.8 Ωm), with low upper-layer resistivity suggestive of pollution.

Lafia Site 1

The geoelectric log for Lafia Site 1 dumpsite VES 1, shown in Figure 6, reveals four layers with inferred lithology, emphasizing thickness and depth ranges: Layer 1 (depth 0–2 m, thickness 2 m, 13.1 Ωm, topsoil), Layer 2 (depth 2–13.1 m, thickness 11.1 m, 175.1 Ωm, sandy clay), Layer 3 (depth 13.1–40.4 m, thickness 27.3 m, 492.6 Ωm, weathered basement), and Layer 4 (depth 40.4–50 m, thickness 9.6 m, 971.9 Ωm, fresh basement). Logs for VES 2, VES 3, and control point VES 4 are in the appendix. Dumpsite VES 2 has four layers: Layer 1 (depth 0–0.4 m, thickness 0.4 m, 25.6 Ωm, topsoil), Layer 2 (depth 0.4–1.6 m, thickness 1.2 m, 7 Ωm, clayey layer), Layer 3 (depth 1.6–6.6 m, thickness 5 m, 204 Ωm, sandy clay), and Layer 4 (depth 6.6–50 m, thickness 43.4 m, 584.8 Ωm, weathered basement); VES 3 has four layers: Layer 1 (depth 0–2.9 m, thickness 2.9 m, 21.6 Ωm, topsoil), Layer 2 (depth 2.9–18.1 m, thickness 15.2 m, 175.5 Ωm, sandy clay), Layer 3 (depth 18.1–45.4 m, thickness 27.3 m, 491.1 Ωm, weathered basement), and Layer 4 (depth 45.4–50 m, thickness 4.6 m, 967 Ωm, fresh basement). The control point VES 4 has four layers: Layer 1 (depth 0–3.3 m, thickness 3.3 m, 72.5 Ωm, topsoil), Layer 2 (depth 3.3–15.2 m, thickness 11.9 m, 135.7 Ωm, sandy clay), Layer 3 (depth 15.2–54.8 m, thickness 39.6 m, 476 Ωm, weathered basement), and Layer 4 (depth 54.8–60 m, thickness 5.2 m, 869.4 Ωm, fresh basement). Dumpsite VES points have thinner upper layers (thickness 0.4–2.9 m vs. 3.3 m for topsoil; 1.2–15.2 m vs. 11.9 m for sandy clay/clayey layer) with lower resistivity (13.1–25.6 Ωm vs. 72.5 Ωm in topsoil; 7–175.5 Ωm vs. 135.7 Ωm in sandy clay/clayey layer), with VES 2's clayey layer (7 Ωm) indicating significant pollution potential.

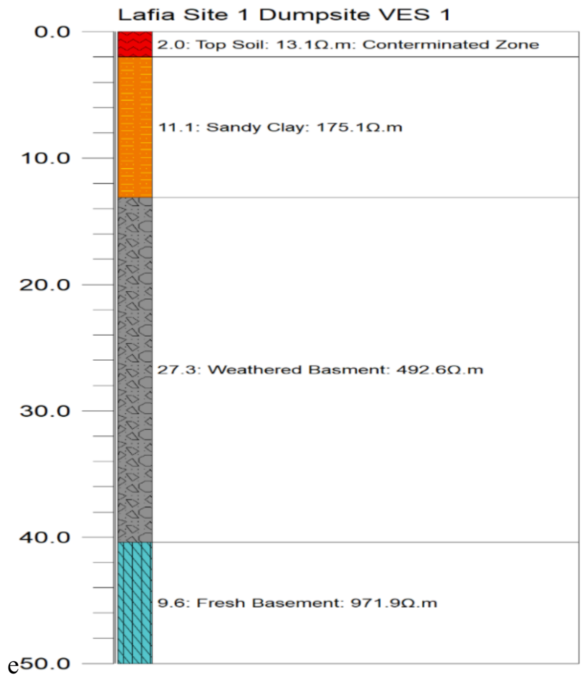

Figure 6: Geoelectric log for Lafia Site 1 dumpsite VES 1

This VES revealed four layers: topsoil (0–2 m, 13.1 Ωm), sandy clay (2–13.1 m, 175.1 Ωm), weathered basement (13.1–40.4 m, 492.6 Ωm), and fresh basement (40.4–50 m, 971.9 Ωm), with low topsoil resistivity indicating potential pollution.

Lafia Site 2

The geoelectric log for Lafia Site 2 dumpsite VES 1, presented in Figure 7, shows four layers with inferred lithology, emphasizing thickness and depth ranges: Layer 1 (depth 0–0.7 m, thickness 0.7 m, 18.2 Ωm, topsoil), Layer 2 (depth 0.7–1.6 m, thickness 0.9 m, 3.7 Ωm, sandy clay), Layer 3 (depth 1.6–54.3 m, thickness 52.7 m, 3706.5 Ωm, fresh basement), and Layer 4 (depth 54.3–60 m, thickness 5.7 m, 2933.3 Ωm, fresh basement). Logs for VES 2, VES 3, and control point VES 4 are in the appendix. Dumpsite VES 2 has four layers: Layer 1 (depth 0–3.3 m, thickness 3.3 m, 31.3 Ωm, topsoil), Layer 2 (depth 3.3–6.5 m, thickness 3.2 m, 36.1 Ωm, sandy clay), Layer 3 (depth 6.5–41.6 m, thickness 35.1 m, 635.8 Ωm, weathered basement), and Layer 4 (depth 41.6–50 m, thickness 8.4 m, 1496.9 Ωm, fresh basement); VES 3 has four layers: Layer 1 (depth 0–2.9 m, thickness 2.9 m, 52.3 Ωm, topsoil), Layer 2 (depth 2.9–8.2 m, thickness 5.3 m, 52.7 Ωm, sandy clay), Layer 3 (depth 8.2–52.6 m, thickness 44.4 m, 552.2 Ωm, weathered basement), and Layer 4 (depth 52.6–60 m, thickness 7.4 m, 1303 Ωm, fresh basement). The control point VES 4 has four layers: Layer 1 (depth 0–0.6 m, thickness 0.6 m, 123.9 Ωm, topsoil), Layer 2 (depth 0.6–10.9 m, thickness 10.3 m, 112.6 Ωm, sandy clay), Layer 3 (depth 10.9–56.8 m, thickness 45.9 m, 472.1 Ωm, weathered basement), and Layer 4 (depth 56.8–60 m, thickness 3.2 m, 1151.9 Ωm, fresh basement). Dumpsite VES points have thinner upper layers (thickness 0.7–3.3 m vs. 0.6 m for topsoil; 0.9–5.3 m vs. 10.3 m for sandy clay) with lower resistivity (18.2–52.3 Ωm vs. 123.9 Ωm in topsoil; 3.7–52.7 Ωm vs. 112.6 Ωm in sandy clay), with VES 1's sandy clay (3.7 Ωm) indicating significant pollution potential.

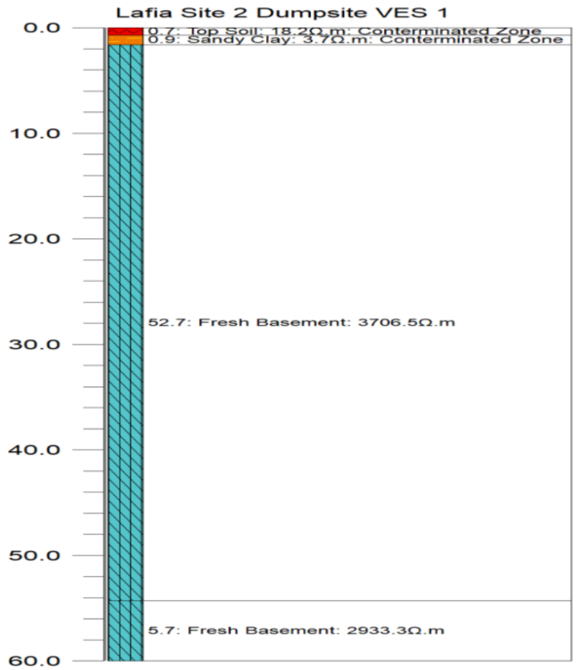

Figure 7: Geoelectric log for Lafia Site 2 dumpsite VES 1

This VES showed four layers: topsoil (0–0.7m, 18.2 Ωm), sandy clay (0.7–1.6 m, 3.7 Ωm), fresh basement (1.6–54.3 m, 3706.5 Ωm), and fresh basement (54.3–60 m, 2933.3 Ωm), with extremely low sandy clay resistivity suggesting significant pollution.

2D Geoelectric and Hole-to-Hole Lithological Models
Nasarawa Toto

The 2D lithological model and hole-to-hole section for the Nasarawa Toto dumpsite (E to E' profile, 40 m total depth), with VES 1 at 0 m, VES 2 at 15 m, and VES 3 at 30 m, are presented in Figure 8 (geoelectric section) and Figure 9 (hole-to-hole section). The model identifies three to four lithological units: topsoil (11.3–18.1 Ωm, depth 0–1.8 m, thickness 0.8–1.8 m), sandy clay (23.7–26.3 Ωm, depth 0.8–8.4 m, thickness 5.5–7.6 m), and fresh basement (924.3–3926.8 Ωm, depth 6.7–40 m, thickness 13.3–33.3 m). Resistivity correlations indicate conductive topsoil and sandy clay (5–100 Ωm) due to contamination, and fresh basement (>1000 Ωm) as resistive bedrock. Compared to the control point VES 4 (appendix: topsoil 106 Ωm, depth 0–1.2 m, thickness 1.2 m; clay 52.3 Ωm, depth 1.2–6.7 m, thickness 5.5 m; fresh basement 8691.4 Ωm, depth 6.7–40 m, thickness 33.3 m), dumpsite VES points show lower resistivity in the topsoil (11.3–18.1 Ωm) and sandy clay (23.7–26.3 Ωm), suggesting contamination.

Spatially, the topsoil thins from 1.8 m at VES 1 to 0.8 m at VES 2, while the sandy clay thickens from 5.5 m at VES 3 to 7.6 m at VES 2, indicating variable sediment deposition. The low-resistivity sandy clay layer (23.7–26.3 Ωm) extends across the 30 m profile, forming a conductive zone for lateral pollutant migration, particularly pronounced at VES 2 (11.3 Ωm in topsoil). The fresh basement's high resistivity (up to 3926.8 Ωm) and thickness (13.3–33.3 m) restrict deeper migration, suggesting remediation efforts should target the upper 8.4 m to mitigate shallow groundwater risks.

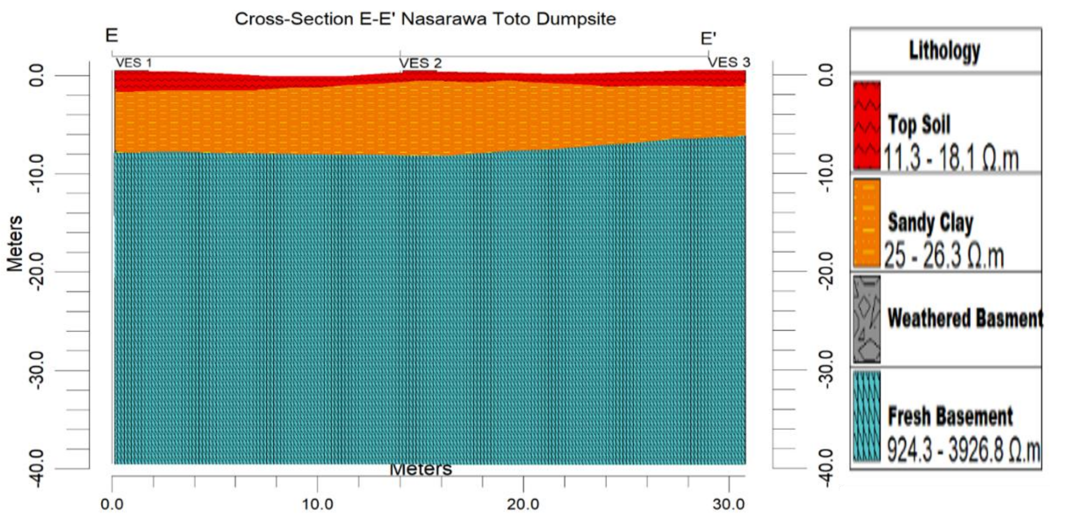

Figure 8: 2D lithological model along E to E' profile (40 m depth) for Nasarawa Toto dumpsite

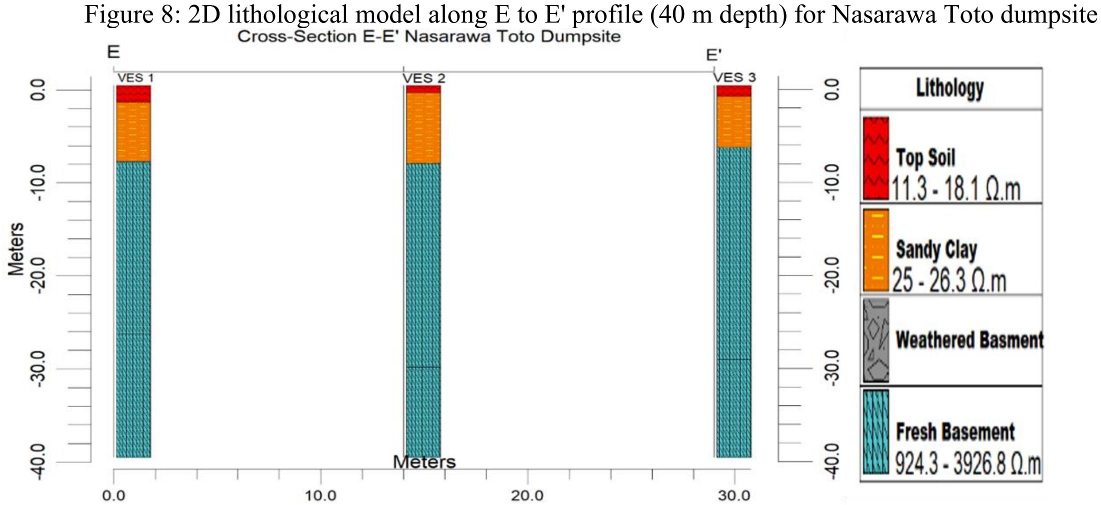

Figure 9: Hole-to-Hole

The topsoil (0–1.8 m, 11.3–18.1 Ωm), sandy clay (0.8–8.4 m, 23.7–26.3 Ωm), and fresh basement (6.7–40 m, 924.3–3926.8 Ωm), with low-resistivity upper layers indicating contamination and potential lateral pollutant migration.

Lafia Site 1

The 2D lithological model and hole-to-hole section for the Lafia Site 1 dumpsite (F to F' profile, 50 m total depth), with VES 1 at 0 m, VES 2 at 15 m, and VES 3 at 30 m, are shown in Figure 10 (geoelectric section) and Figure 10 (hole-to-hole section). The model delineates four lithological units: topsoil (13.1–25.6 Ωm, depth 0–2.9 m, thickness 0.4–2.9 m), sandy clay/clayey layer (7–175.5 Ωm, depth 0.4–18.1 m, thickness 1.2–15.2 m), weathered basement (204–584.8 Ωm, depth 1.6–45.4 m, thickness 5–43.4 m), and fresh basement (967–971.9 Ωm, depth 40.4–50 m, thickness 4.6–9.6 m). Resistivity correlations indicate conductive topsoil and sandy clay/clayey layers (5–100 Ωm) due to contamination, weathered basement (100–1000 Ωm) as altered rock, and fresh basement (>1000 Ωm) as resistive bedrock. Compared to the control point VES 4 (appendix: topsoil 72.5 Ωm, depth 0–3.3 m, thickness 3.3 m; sandy clay 135.7 Ωm, depth 3.3–15.2 m, thickness 11.9 m; weathered basement 476 Ωm, depth 15.2–54.8 m, thickness 39.6 m; fresh basement 869.4 Ωm, depth 54.8–60 m, thickness 5.2 m), dumpsite VES points show lower resistivity, with VES 2's clayey layer (7 Ωm) indicating significant contamination.

Spatially, the topsoil thickens from 0.4 m at VES 2 to 2.9 m at VES 3, while the sandy clay/clayey layer varies significantly from 1.2 m at VES 2 to 15.2 m at VES 3, suggesting variable sediment thickness. The low-resistivity clayey layer at VES 2 (7 Ωm) forms a localized contamination zone at 15 m, facilitating lateral pollutant migration. The fresh basement's thickness (4.6–9.6 m) restricts deeper migration, indicating remediation should focus on the upper 18.1 m to protect shallow groundwater.

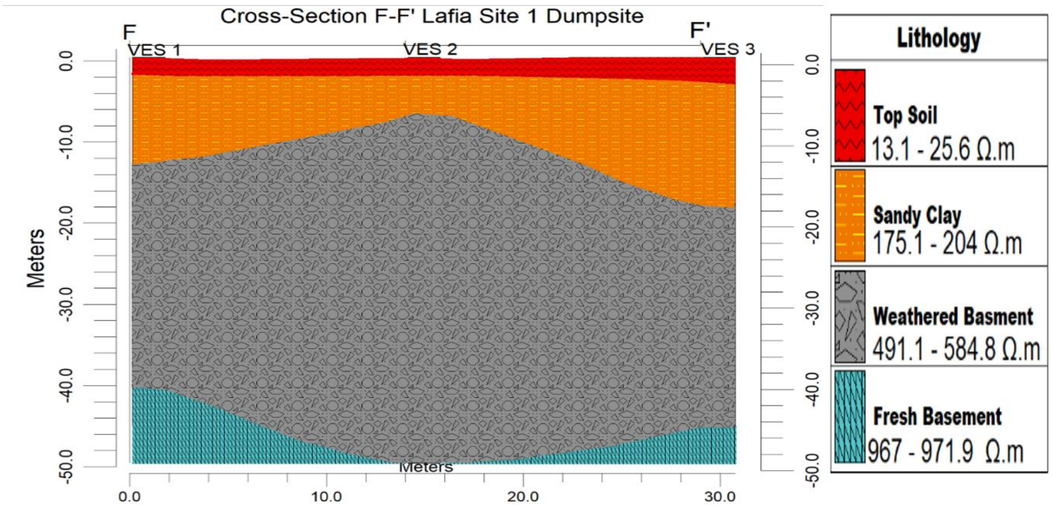

Figure 10: 2D Lithological Model along F to F' profile (50 m depth) for Lafia Site 1 Dumpsite

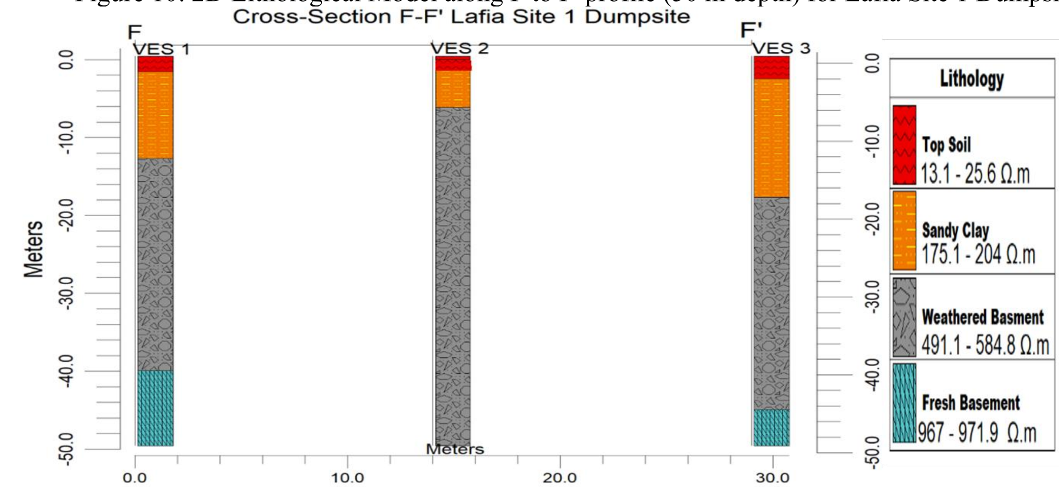

Figure 11: Hole-to-Hole

The topsoil (0–2.9 m, 13.1–25.6 Ωm), sandy clay/clayey layer (0.4–18.1 m, 7–175.5 Ωm), weathered basement (1.6–45.4 m, 204–584.8 Ωm), and fresh basement (40.4–50 m, 967–971.9 Ωm), with low-resistivity clayey layer at VES 2 indicating localized contamination.

Lafia Site 2

The 2D lithological model and hole-to-hole section for the Lafia Site 2 dumpsite (G to G' profile, 60 m total depth), with VES 1 at 0 m, VES 2 at 15 m, and VES 3 at 30 m, are presented in Figure 12 (geoelectric section) and Figure 13 (hole-to-hole section). The model identifies four lithological units: topsoil (18.2–52.3 Ωm, depth 0–3.3 m, thickness 0.7–3.3 m), sandy clay (3.7–52.7 Ωm, depth 0.7–8.2 m, thickness 0.9–5.3 m), weathered basement (552.2–635.8 Ωm, depth 6.5–52.6 m, thickness 35.1–44.4 m), and fresh basement (1303–3706.5 Ωm, depth 41.6–60 m, thickness 5.7–8.4 m). Resistivity correlations indicate conductive topsoil and sandy clay (5–100 Ωm) due to contamination, weathered basement (100–1000 Ωm) as altered rock, and fresh basement (>1000 Ωm) as resistive bedrock. Compared to the control point VES 4 (appendix: topsoil 123.9 Ωm, depth 0–0.6 m, thickness 0.6 m; sandy clay 112.6 Ωm, depth 0.6–10.9 m, thickness 10.3 m; weathered basement 472.1 Ωm, depth 10.9–56.8 m, thickness 45.9 m; fresh basement 1151.9 Ωm, depth 56.8–60 m, thickness 3.2 m), dumpsite VES points show significantly lower resistivity, with VES 1's sandy clay (3.7 Ωm) indicating severe contamination.

Spatially, the topsoil thickens from 0.7 m at VES 1 to 3.3 m at VES 2, while the sandy clay varies from 0.9 m at VES 1 to 5.3 m at VES 3. The extremely low-resistivity sandy clay at VES 1 (3.7 Ωm) forms a major contamination zone at the profile's start, facilitating lateral pollutant migration across the 30 m profile. The fresh basement's high resistivity (up to 3706.5 Ωm) and thickness (5.7–8.4 m) limit deeper migration, suggesting remediation should target the upper 8.2 m to prevent shallow groundwater contamination.

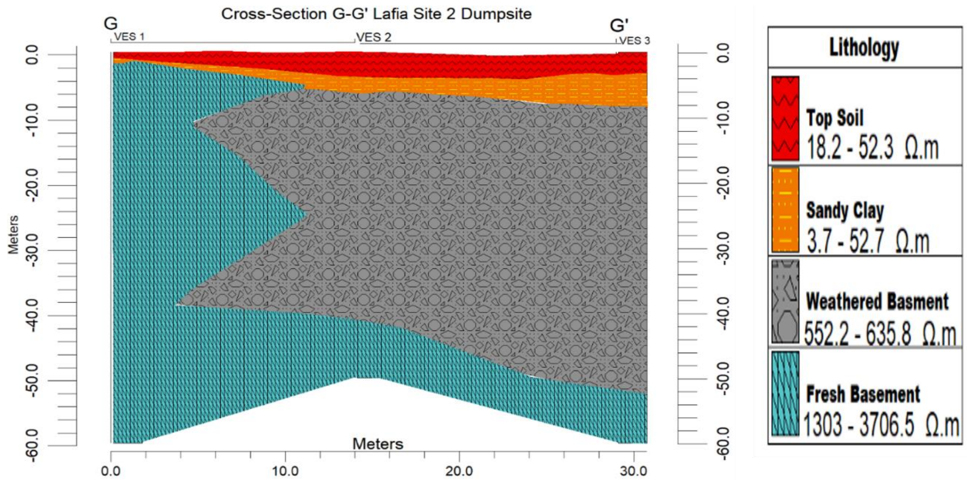

Figure 12: 2D Lithological Model Along G To G' Profile (60 m depth) for Lafia Site 2 Dumpsite

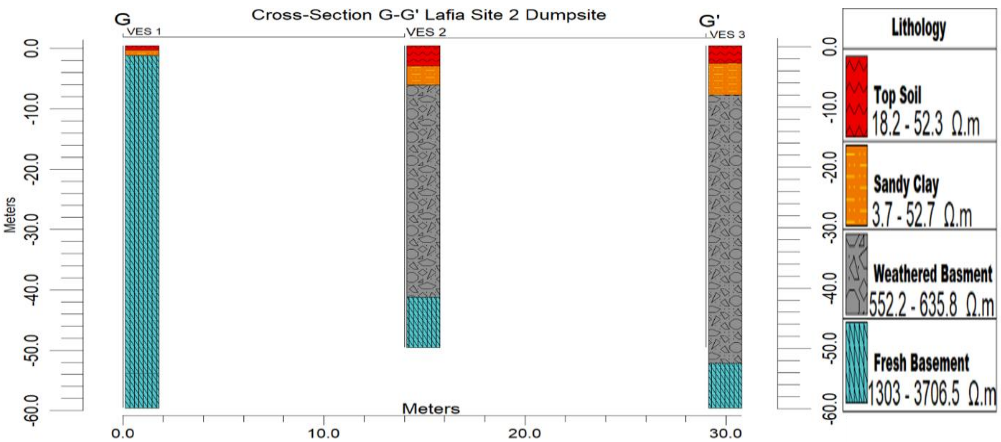

Figure 13: Hole-to-Hole

The topsoil (0–3.3 m, 18.2–52.3 Ωm), sandy clay (0.7–8.2 m, 3.7–52.7 Ωm), weathered basement (6.5–52.6 m, 552.2–635.8 Ωm), and fresh basement (41.6–60 m, 1303–3706.5 Ωm), with extremely low-resistivity sandy clay at VES 1 indicating severe contamination and lateral pollutant migration.

Pseudo-Sections for Subsurface Apparent Resistivity Distribution and Contamination Assessment

Nasarawa Toto

The pseudo-section for Nasarawa Toto (E to E' profile, 40 m depth), shown in Figure 14, is constructed from VES 1 (0 m), VES 2 (15 m), and VES 3 (30 m). It displays apparent resistivity variations: topsoil (11.3–18.1 Ωm, depth 0–1.8 m, blue), sandy clay (23.7–26.3 Ωm, depth 0.8–8.4 m, blue), and fresh basement (924.3–3926.8 Ωm, depth 6.7–40 m, pink). The low apparent resistivity in the topsoil (11.3–18.1 Ωm) and sandy clay (23.7–26.3 Ωm), particularly at VES 2 (11.3 Ωm topsoil, 26.3 Ωm sandy clay), forms blue zones indicative of conductive anomalies, likely due to leachate contamination. Compared to the control point VES 4 (appendix: topsoil 106 Ωm, depth 0–1.2 m; clay 52.3 Ωm, depth 1.2–6.7 m; fresh basement 8691.4 Ωm, depth 6.7–40 m), the dumpsite's upper layers (0–8.4 m) show significantly lower resistivity. The blue zones extend across the 30 m profile, suggesting a continuous pathway for lateral pollutant migration, particularly at 15 m (VES 2). The pink fresh basement (up to 3926.8 Ωm) restricts deeper migration. The pseudo-section complements the lithological model by visualizing the conductive zone in the upper 8.4 m, critical for remediation planning.

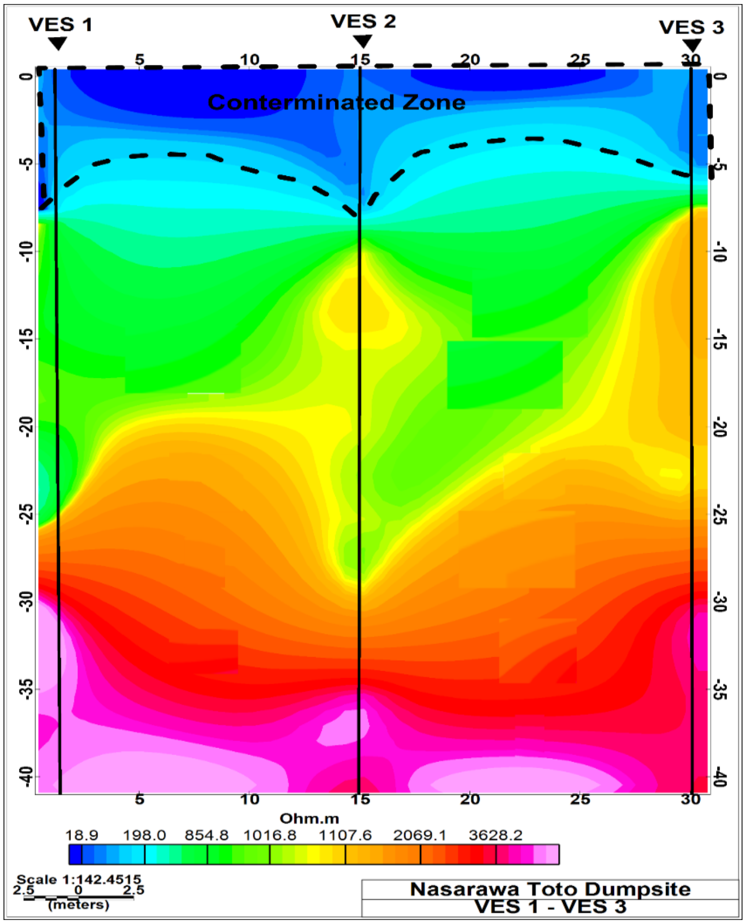

Figure 14: Pseudo-section for Nasarawa Toto (E to E' profile, 40 m depth)

The blue low-resistivity zones (11.3–18.1 Ωm topsoil, 0–1.8 m; 23.7–26.3 Ωm sandy clay, 0.8–8.4 m) indicating leachate contamination, and pink fresh basement (924.3–3926.8 Ωm, 6.7–40 m) as a resistive barrier across the 30 m profile.

Lafia Site 1

The pseudo-section for Lafia Site 1 (F to F' profile, 50 m depth), shown in Figure 15, is derived from VES 1 (0 m), VES 2 (15 m), and VES 3 (30 m). It displays apparent resistivity variations: topsoil (13.1–25.6 Ωm, depth 0–2.9 m, blue), sandy clay/clayey layer (7–175.5 Ωm, depth 0.4–18.1 m, blue to green), weathered basement (204–584.8 Ωm, depth 1.6–45.4 m, green to yellow), and fresh basement (967–971.9 Ωm, depth 40.4–50 m, pink). The extremely low apparent resistivity at VES 2 (7 Ωm in clayey layer, depth 0.4–1.6 m) forms an intense blue zone, indicating a significant conductive anomaly likely due to leachate contamination. Compared to the control point VES 4 (appendix: topsoil 72.5 Ωm, depth 0–3.3 m; sandy clay 135.7 Ωm, depth 3.3–15.2 m; weathered basement 476 Ωm, depth 15.2–54.8 m; fresh basement 869.4 Ωm, depth 54.8–60 m), the dumpsite's upper layers (0–18.1 m) show markedly lower resistivity. The blue-to-green zone in the sandy clay/clayey layer extends across the 30 m profile, suggesting a major pathway for lateral pollutant migration, particularly at 15 m (VES 2). The pink fresh basement (967–971.9 Ωm) limits deeper migration. The pseudo-section enhances the lithological model by highlighting the localized severe contamination zone in the upper 18.1 m.

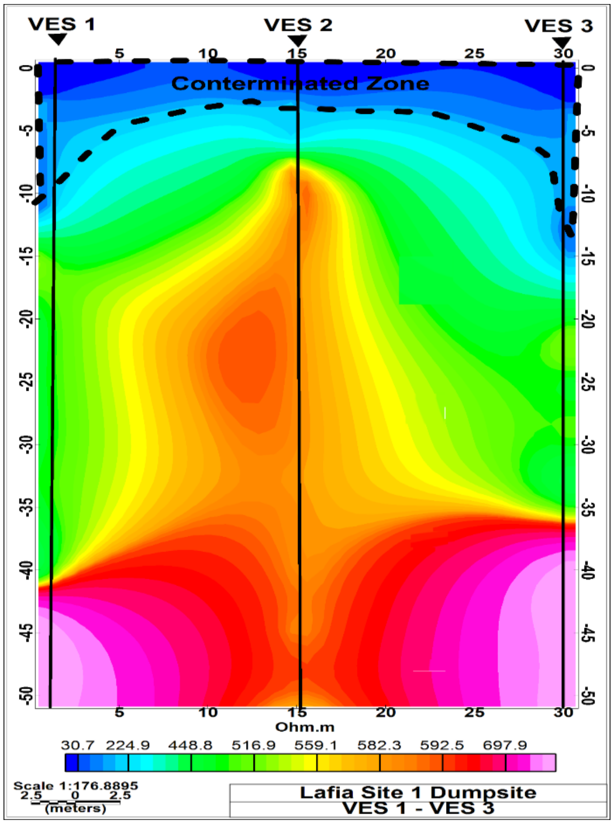

Figure 15: Pseudo-section for Lafia Site 1 (F to F' profile, 50 m depth)

The blue low-resistivity zones (13.1–25.6 Ωm topsoil, 0–2.9 m; 7–175.5 Ωm sandy clay/clayey layer, 0.4–18.1 m) with severe contamination at VES 2, green to yellow weathered basement (204–584.8 Ωm, 1.6–45.4 m), and pink fresh basement (967–971.9 Ωm, 40.4–50 m) across the 30 m profile.

Lafia Site 2

The pseudo-section for Lafia Site 2 (G to G' profile, 60 m depth), shown in Figure 16, is constructed from VES 1 (0 m), VES 2 (15 m), and VES 3 (30 m). It displays apparent resistivity variations: topsoil (18.2–52.3 Ωm, depth 0–3.3 m, blue), sandy clay (3.7–52.7 Ωm, depth 0.7–8.2 m, blue), weathered basement (552.2–635.8 Ωm, depth 6.5–52.6 m, green to yellow), and fresh basement (1303–3706.5 Ωm, depth 41.6–60 m, pink). The extremely low apparent resistivity in the sandy clay at VES 1 (3.7 Ωm, depth 0.7–1.6 m) forms an intense blue zone, indicating severe conductive anomalies likely due to leachate contamination. Compared to the control point VES 4 (appendix: topsoil 123.9 Ωm, depth 0–0.6 m; sandy clay 112.6 Ωm, depth 0.6–10.9 m; weathered basement 472.1 Ωm, depth 10.9–56.8 m; fresh basement 1151.9 Ωm, depth 56.8–60 m), the dumpsite's upper layers (0–8.2 m) show significantly lower resistivity. The blue zone in the sandy clay extends across the 30 m profile, suggesting a significant pathway for lateral pollutant migration, particularly at 0 m (VES 1). The pink fresh basement (1303–3706.5 Ωm) restricts deeper migration. The pseudo-section enhances the lithological model by highlighting the severe conductive anomaly in the upper 8.2 m, critical for remediation planning.

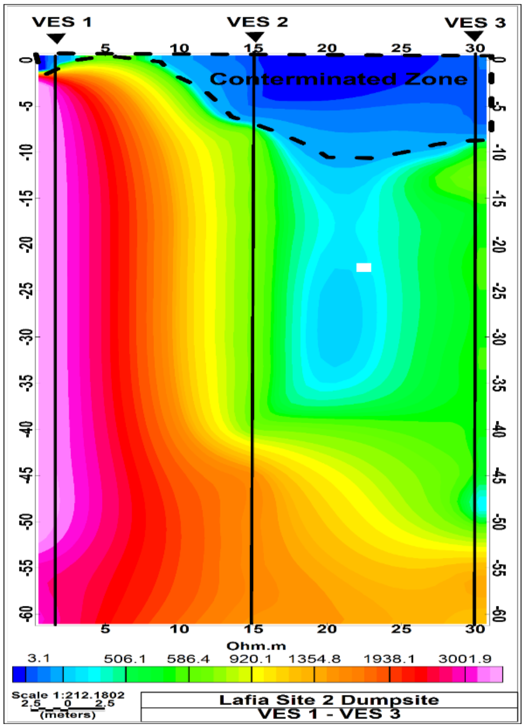

Figure 16: Pseudo-section for Lafia Site 2 (G to G' profile, 60 m depth)

The intense blue low-resistivity zones (18.2–52.3 Ωm topsoil, 0–3.3 m; 3.7–52.7 Ωm sandy clay, 0.7–8.2 m) with severe contamination at VES 1, green to yellow weathered basement (552.2–635.8 Ωm, 6.5–52.6 m), and pink fresh basement (1303–3706.5 Ωm, 41.6–60 m) across the 30 m profile.

Results of Water Analysis

Table 1: Physico-chemical Analysis of Water Samples – Nassarawa Toto and Control

S/No	Parameters	Control	Dump Site
1	Cr(mg/l)	0.1341	0.7800
2	K(mg/l)	7.5706	11.6000
3	Ca(mg/l)	3.2060	8.0000
4	Ni(mg/l)	0.0989	1.2900
5	Mg(mg/l)	4.6894	5.0000
6	Mn(mg/l)	0.2567	1.3100
7	Na(mg/l)	10.0083	8.1000
8	Cu(mg/l)	-0.2506	0.8600
9	Cd(mg/l)	0.0262	1.0200
10	Co(mg/l)	0.3533	0.8800
11	Pb(mg/l)	0.7228	0.0072
12	Fe(mg/l)	0.4938	0.4900
13	Zn(mg/l)	0.2013	0.4000
14	Turbidity (NTU)	0.8000	0.2000
15	Conductivity(us/cm)	241.5000	0.2000
16	pH	5.1400	5.9000
17	TSS (mg/l)	5.0400	19.9900
18	DO (mg/l)	9.4500	9.0000
19	Chloride(mg/l)	23.8400	3.9900
20	Phosphate(mg/l)	1.1100	6.1400
21	Sulphate(mg/l)	0.0300	0.0500
22	Nitrate(mg/l)	0.6400	0.0056
23	Hardness(mg/l)	3.8000	4.2000

Analysis and Interpretation of Water Sample Results Nassarawa Toto

The analysis of water samples collected from Nassarawa Toto reveals significant variations between the control site and the dump-site area (Table 1), suggesting varying degrees of contamination likely linked to leachate infiltration from waste disposal activities. Heavy metal concentrations provide the clearest indication of pollution influence. Chromium (Cr), for instance, shows a notable increase from 0.134 mg/L at the control site to 0.78 mg/L at the dump site, exceeding most drinking-water guideline limits (<0.05 mg/L). This rise suggests direct input from metallic waste, batteries, or industrial residues. Similarly, Nickel (Ni) increases sharply from 0.098 mg/L to 1.29 mg/L, indicating strong contamination likely associated with corrosion of metallic components or electronic waste. Manganese (Mn) also rises significantly from 0.256 mg/L to 1.31 mg/L, consistent with groundwater impacted by organic leachate and reducing conditions.

Other metals such as Cadmium (Cd) and Copper (Cu) show marked increases, with Cd rising from 0.026 mg/L to 1.02 mg/L, far exceeding acceptable limits (<0.003 mg/L). This indicates severe contamination, as cadmium is commonly associated with plastics, pigments, and battery degradation. Copper rises to 0.86 mg/L, compared to negligible or negative baseline values at the control site, further supporting the presence of anthropogenic pollution. Conversely, Lead (Pb) shows an unexpected drop from 0.722 mg/L at the control site to 0.0072 mg/L at the dump site. This anomaly may be due to adsorption of Pb onto soil particles, precipitation, or different geochemical conditions limiting mobility.

General water chemistry parameters also reveal important variations. Total Suspended Solids (TSS) increases substantially from 5.04 mg/L to 19.99 mg/L, suggesting higher particulate loads, possibly due to erosion or solid waste runoff. Conversely, chloride concentration decreases from 23.84 mg/L to 3.99 mg/L, indicating that chloride pollution is not a major component of the dump-site leachate, or it may be subject to dilution. Phosphate increases sharply from 1.11 mg/L to 6.14 mg/L, most likely due to decomposition of organic waste, detergents, and food residues. The pH rises moderately from 5.14 to 5.9, indicating slightly less acidic conditions near the dump site, possibly because of buffering by mineral-rich waste.

Some parameters decline rather than increase. Sodium (Na) decreases slightly from 10.0 mg/L to 8.1 mg/L, suggesting limited influence of domestic waste salts. Turbidity drops from 0.8 NTU to 0.2 NTU, and conductivity shows an unusual extreme reduction from 241.5 µS/cm at the control site to 0.2 µS/cm at the dump site, an unlikely result that may indicate sampling or instrument error rather than true water chemistry. Dissolved oxygen (DO) reduces slightly from 9.45 mg/L to 9.0 mg/L, consistent with mild microbial activity but not typical of heavy organic pollution.

finally, the results reveal that the dump-site water is mainly contaminated by toxic heavy metals, particularly Cr, Ni, Mn, Cd, and Cu and phosphate, indicating a clear influence of waste leachate on groundwater chemistry. The magnitude of contamination in several parameters exceeds WHO and national drinking-water standards, posing significant risks to human health if consumed untreated. These findings emphasize the need for improved waste-management practices, continuous groundwater monitoring, and possible remediation measures in Nassarawa Toto to protect surrounding communities.

Table 2: Physico-chemical Analysis of Water Samples – Lafia 1 and Control

S/No	Parameters	Control BH Near Dumpsite	Dump Site
1	Cr(mg/l)	0.0023	0.0235
2	K(mg/l)	6.5000	162.5900
3	Ca(mg/l)	0.0001	8.0000
4	Ni(mg/l)	1.6180	1.6650
5	Mg(mg/l)	3.7000	7.0000
6	Mn(mg/l)	1.2780	1.4280
7	Na(mg/l)	6.3900	78.2380
8	Cu(mg/l)	0.0012	0.5190
9	Cd(mg/l)	0.9230	1.2320
10	Co(mg/l)	1.8290	2.6690
11	Pb(mg/l)	3.5000	1.1790
12	Fe(mg/l)	0.6000	1.1780
13	Zn(mg/l)	0.6480	0.2685
14	Turbidity (NTU)	1.3000	2.7000
15	Conductivity(us/cm)	97.6000	431.0000
16	Ph	7.5000	8.0900
17	TSS (mg/l)	76.6000	2.1200
18	DO (mg/l)	10.0000	10.0000

19	Chloride(mg/l)	78.5000	351.0000
20	Phosphate(mg/l)	6.1000	4.9500
21	Sulphate(mg/l)	0.0200	0.0600
22	Nitrate(mg/l)	6.8500	187.2500
23	Hardness(mg/l)	4.0000	6.0000

Analysis and Interpretation of Water Sample Results From Lafia 1

The results from the Lafia 1 groundwater sample show significant variation between the control borehole (BH) and the borehole near the dumpsite, suggesting strong influence of leachate infiltration on groundwater chemistry (Table 2). Heavy metals, major ions, and physicochemical parameters indicate clear patterns of contamination attributable to waste decomposition processes and pollutant transport through the soil profile.

Chromium (Cr) concentrations rise from 0.0023 mg/L in the control to 0.0235 mg/L at the dumpsite. Although the absolute values appear moderate, the tenfold increase implies leachate-induced mobilization of Cr, potentially from discarded metal scraps, dyes, or batteries. Persistent exposure poses risks of kidney and liver toxicity.

Potassium (K) shows an extreme increase from 6.5 mg/L to 162.59 mg/L, indicating severe contamination. High K levels typically originate from organic waste decomposition, fertilizers, and ash residues. This spike is a clear marker of leachate intrusion.

Calcium (Ca) increases drastically from trace amounts (0.00012 mg/L) to 8 mg/L near the dumpsite. This suggests dissolution of calcareous waste materials or leachate enrichment from biodegradable waste, though levels remain within potable limits.

Nickel (Ni) rises slightly (1.618 to 1.665 mg/L), showing moderate contamination. However, both values exceed WHO limits (0.02 mg/L), making the groundwater unsafe and indicating industrial or metallic waste contributions.

Magnesium (Mg) levels double (3.7 to 7 mg/L), likely reflecting mineral dissolution or input from household waste and metals. While not excessively high, the increase supports evidence of leachate infiltration.

Manganese (Mn) shows a similar pattern (1.278 to 1.428 mg/L), exceeding recommended limits (0.4 mg/L). High Mn can impair neurological development with prolonged exposure.

Sodium (Na) demonstrates a major rise from 6.39 mg/L to 78.238 mg/L. This substantial increase indicates saline leachate flow and decomposition of sodium-rich waste such as food scraps and detergents.

Copper (Cu) increases from 0.00123 mg/L to 0.519 mg/L, likely from corroded metals and electronic waste. Elevated copper can cause gastrointestinal irritation and metallic taste.

Cadmium (Cd) increases from 0.923 to 1.232 mg/L, extremely high and dangerous. Cadmium is a highly toxic metal linked to kidney failure, bone deformation (Itai-itai disease), and carcinogenic effects. Its presence suggests batteries, plastics, and pigments in the waste stream.

Cobalt (Co) rises sharply (1.829 to 2.669 mg/L), indicating contamination from alloys, paints, and industrial waste. Consuming such water poses cardiovascular and metabolic risks.

Lead (Pb) decreases from 3.5 mg/L (control) to 1.179 mg/L (dumpsite). Though the dumpsite value is lower, both values are dangerously above WHO limits (0.01 mg/L). Pb contamination indicates widespread pollution from pipes, batteries, and paints.

Iron (Fe) nearly doubles (0.6 to 1.178 mg/L), indicating leachate interaction with soils and corroded materials. High Fe affects taste and color but also signals poor groundwater protection.

Zinc (Zn) decreases from 0.648 mg/L to 0.2685 mg/L, suggesting dilution or preferential mobility of other metals. Both values remain within safe limits.

Turbidity rises from 1.3 NTU to 2.7 NTU, reflecting increased particulate matter due to waste infiltration, posing microbiological risks.

Electrical Conductivity increases significantly (97.6 to 431 µS/cm), indicating higher dissolved solids and ionic contamination—strong evidence of leachate penetration.

pH shifts from 7.5 (neutral) to 8.09 (slightly alkaline), likely due to ammonia, detergents, and decomposition byproducts.

Total Suspended Solids (TSS) decreases dramatically (76.6 mg/L to 2.12 mg/L), indicating filtration or soil attenuation, though high TSS in the control suggests local sediment contamination unrelated to the dump.

Dissolved Oxygen (DO) remains constant at 10 mg/L, showing good aeration but not reflecting chemical contamination levels.

Chloride increases sharply (78.5 to 351 mg/L), a strong signature of organic and inorganic leachate contamination. High Cl^- can corrode pipes and alter taste.

Phosphate decreases (6.1 to 4.95 mg/L), though values still reflect contamination from detergents and organic waste.

Sulphate increases slightly (0.02 to 0.06 mg/L), suggesting mild influence of biodegradable waste.

Nitrate surges from 6.85 mg/L to 187.25 mg/L—dangerously high and indicative of sewage, fertilizers, and organic waste. High nitrate can cause methemoglobinemia ("blue baby syndrome") and other health issues.

Hardness increases mildly (4 to 6 mg/L), showing low mineral hardness overall.

The Lafia 1 groundwater near the dumpsite shows severe contamination, especially with heavy metals (Cd, Pb, Ni, Co), salts (Na, Cl), nutrients (nitrate), and high conductivity, clearly demonstrating strong leachate infiltration. Many parameters exceed WHO drinking water standards, making the dumpsite water unsafe for human consumption and indicating an urgent need for ground.

Table 3: Physico-chemical Analysis of Water Samples – Lafia 2 and Control

S/No	Parameters	Control BH Near Dumpsite	Dump Site
1	Cr(mg/l)	0.0023	0.0001
2	K(mg/l)	6.5000	167.5250
3	Ca(mg/l)	0.0001	11.0000
4	Ni(mg/l)	1.6180	0.0756
5	Mg(mg/l)	3.7000	6.0000
6	Mn(mg/l)	1.2780	2.5650
7	Na(mg/l)	6.3900	76.5000
8	Cu(mg/l)	0.0012	0.5345
9	Cd(mg/l)	0.9230	0.6880
10	Co(mg/l)	1.8290	2.5680
11	Pb(mg/l)	3.5000	2.2790
12	Fe(mg/l)	0.6000	1.2240
13	Zn(mg/l)	0.6480	0.0021
14	Turbidity (NTU)	1.3000	680.0000
15	Conductivity(us/cm)	97.6000	394.3000
16	pH	7.5000	7.6000
17	TSS (mg/l)	76.6000	19.5000
18	DO (mg/l)	10.0000	13.0000
19	Chloride(mg/l)	78.5000	553.8900
20	Phosphate(mg/l)	6.1000	5.8900
21	Sulphate(mg/l)	0.0200	0.0550
22	Nitrate(mg/l)	6.8500	142.0000
23	Hardness(mg/l)	4.0000	8.0000

Analysis and Interpretation of Water Sample Results - Lafia 2

The water sample results from the Lafia 2 location show significant variations between the control borehole and the borehole situated near the dumpsite, revealing the influence of leachate contamination of groundwater chemistry (Table 3). A detailed parameter-by-parameter analysis provides insight into the extent of pollution and its potential public-health implications.

Chromium (Cr)

Chromium levels reduce drastically from 0.0023 mg/L in the control to 0.0001 mg/L at the dumpsite. This decrease suggests that the dumpsite does not release chromium into the groundwater at this point, or that reducing conditions in the subsurface may immobilize Cr through precipitation.

Potassium (K)

Potassium increases sharply from 6.5 mg/L to 167.525 mg/L, indicating strong contamination from organic waste, ash residues, food waste, and decomposed plant matter. Potassium is a major component of landfill leachate and an indicator of fresh organic pollution.

Calcium (Ca)

Calcium rises from 0.00012 mg/L to 11 mg/L, showing enrichment from leachate containing cement debris, soil dissolution, and construction materials. Elevated Ca often marks early leachate infiltration.

Nickel (Ni)

Nickel concentration drops significantly from 1.618 mg/L to 0.0756 mg/L at the dumpsite borehole. This may reflect adsorption of Ni onto clay minerals or organic matter in refuse layers, reducing its mobility.

Magnesium (Mg)

Magnesium increases from 3.7 mg/L to 6 mg/L, reflecting mineral dissolution and infiltration of leachate enriched with Mg from metals, batteries, and dissolved soil materials.

Manganese (Mn)

Mn increases from 1.278 mg/L to 2.565 mg/L, suggesting reducing groundwater conditions near the dumpsite which mobilize manganese from soil and waste materials. Elevated Mn is associated with neurological risks when consumed chronically.

Sodium (Na)
Sodium rises from 6.39 mg/L to 76.5 mg/L, confirming intrusion of highly soluble salts from the dumpsite. Na elevation is a typical signature of leachate impact.

Copper (Cu)
Cu increases significantly from 0.00123 mg/L to 0.5345 mg/L, indicating contamination from corroded pipes, metallic waste, and electronic scraps.

Cadmium (Cd)
Cd decreases from 0.923 mg/L to 0.688 mg/L, but both values are dangerously high and far above WHO standards (0.003 mg/L). This indicates serious contamination from batteries, pigments, plastics, and disposed electronics.

Cobalt (Co)
Cobalt rises from 1.829 mg/L to 2.568 mg/L, indicating input from metal alloys, dyes, and rechargeable batteries. Elevated Co poses toxicological concern.

Lead (Pb)
Lead drops from 3.5 mg/L (control) to 2.279 mg/L, but both remain critically above permissible limits (0.01 mg/L). The high levels indicate chronic leachate impact and local geology possibly rich in Pb-bearing minerals.

Iron (Fe)
Iron increases from 0.6 mg/L to 1.224 mg/L, suggesting increased reducing conditions and leachate-soil interactions releasing Fe into groundwater.

Zinc (Zn)
Zinc decreases dramatically from 0.648 mg/L to 0.00211 mg/L, likely due to adsorption or precipitation under prevailing groundwater chemistry.

Turbidity
Turbidity rises sharply from 1.3 NTU to 680 NTU, showing extreme particulate and colloidal contamination from leachate, severely compromising potability.

Electrical Conductivity (EC)
EC increases from 97.6 µS/cm to 394.3 µS/cm, confirming increased ionic concentration and strong leachate impact.

pH
pH shifts slightly from 7.5 to 7.6, indicating a stable near-neutral to slightly alkaline environment. This range supports mobility of some metals (e.g., Co, Mn).

Total Suspended Solids (TSS)
TSS decreases from 76.6 mg/L to 19.5 mg/L, possibly reflecting settling of particles or difference in sampling conditions. However, the dumpsite value is still above acceptable limits.

Dissolved Oxygen (DO)
DO increases from 10 to 13 mg/L, possibly due to photosynthetic activity or aeration during sampling. Elevated DO does not reflect good water quality in this context because chemical contamination remains severe.

Chloride (Cl^-)
Chloride rises sharply from 78.5 mg/L to 553.89 mg/L, confirming strong influence of domestic waste, salt leachates, and organic decomposition.

Phosphate (PO_4^{3-})
Phosphate decreases slightly from 6.1 mg/L to 5.89 mg/L, both values elevated, indicating contamination from detergents, food waste, and organic decomposition.

Sulphate
Slight increase from 0.02 mg/L to 0.055 mg/L, showing mild sulphate enrichment, typical of leachate from industrial and food wastes.

Nitrate
Nitrate increases extremely from 6.85 mg/L to 142 mg/L, indicating contamination from organic waste, decayed vegetation, animal remains, and nitrogen-rich household waste. High nitrate levels pose severe health risks, especially to infants (methemoglobinemia).

Hardness
Total hardness increases from 4 mg/L to 8 mg/L, indicating slightly more mineralized groundwater, though still soft water.
The Lafia 2 dumpsite water sample shows clear, strong evidence of leachate contamination, with extremely elevated levels of potassium, sodium, chloride, nitrate, copper, cobalt, manganese, and electrical conductivity. The high turbidity (680 NTU) further demonstrates heavy intrusion of suspended solids. Several toxic heavy metals (Pb, Cd, Ni, Cu, Co) are present in unsafe concentrations, exceeding WHO drinking water guidelines. The results reflect severe deterioration of groundwater quality due to dumpsite activities, posing significant health risks such as kidney damage, neurological disorders, cancer, and gastrointestinal illnesses. Immediate intervention measures, including groundwater protection, dumpsite containment, and provision of alternative water sources, are urgently required.

Discussions
Subsurface Characterization
The geoelectric and lithological characteristics inferred from vertical electrical sounding (VES) data across the

seven dumpsite locations, Nasarawa Toto, Lafia Site 1, and Lafia Site 2 reveal consistent subsurface layering with distinct resistivity signatures, as detailed in the geoelectric logs and pseudo-sections. The VES data, collected at VES 1 (0 m), VES 2 (15 m), and VES 3 (30 m) along 30 m profiles, extend to depths of 50 m (Lafia Site 1), 60 m (Lafia Site 2), and 40 m (Nasarawa Toto). The subsurface typically comprises four layers, except for Nasarawa Toto VES 2–3 shows three layers: topsoil (0–3.6 m, 6.2–68.7 Ωm), sandy clay or clayey layer (0.4–18.1 m, 3.7–175.5 Ωm), weathered basement (1.6–52.6 m, 21.4–895.2 Ωm), and fresh basement (3.4–60 m, 758.6–11811.7 Ωm). These layers were inferred using WinResist modeling, correlating resistivity ranges with lithology: low resistivity (5–100 Ωm) for topsoil and sandy clay indicates conductive, potentially saturated or contaminated sediments; moderate resistivity (100–1000 Ωm) for weathered basement reflects partially altered rock; and high resistivity (>1000 Ωm) for fresh basement signifies unweathered bedrock.

Nasarawa Toto has topsoil (0.8–1.8 m, 11.3–18.1 Ωm), sandy clay (5.5–7.6 m, 23.7–26.3 Ωm), and fresh basement (13.3–33.3 m, 924.3–3926.8 Ωm), less resistive than the control point (topsoil: 1.2 m, 106 Ωm; clay: 5.5 m, 52.3 Ωm). Lafia Site 1 shows topsoil (0.4–2.9 m, 13.1–25.6 Ωm), sandy clay/clayey layer (1.2–15.2 m, 7–175.5 Ωm), and weathered basement (5–43.4 m, 204–584.8 Ωm), contrasting with the control point (topsoil: 3.3 m, 72.5 Ωm; sandy clay: 11.9 m, 135.7 Ωm). Lafia Site 2 has topsoil (0.7–3.3 m, 18.2–52.3 Ωm), sandy clay (0.9–5.3 m, 3.7–52.7 Ωm), and weathered basement (35.1–44.4 m, 552.2–635.8 Ωm), less resistive than the control point (topsoil: 0.6 m, 123.9 Ωm; sandy clay: 10.3 m, 112.6 Ωm).

The inferred lithologies align with the geological context of the study area, likely within the Basement Complex of North-Central Nigeria, characterized by weathered and fresh basement rocks (e.g., granite, gneiss) overlain by thin sedimentary cover (e.g., sandy clay, topsoil). The topsoil and sandy clay reflect alluvial or residual soils common in tropical regions, while the weathered basement indicates saprolite, and the fresh basement corresponds to unweathered crystalline rock. Dumpsite VES points consistently show thinner, less resistive upper layers compared to control points, suggesting disturbance from waste and leachate infiltration, while deeper layers maintain high resistivity, consistent with regional bedrock.

The geoelectric investigation of Nasarawa Toto reveals a subsurface configuration that is largely consistent with the typical regolith development found across the Nigerian Basement Complex. The data indicates that the subsurface typically comprises four distinct geoelectric layers, representing a standard evolutionary sequence from topsoil to fresh crystalline basement (Chiazor et al., 2024). However, a localized variation occurs at VES 2–3, which exhibits a three-layer model. This transition between three- and four-layer configurations is a documented phenomenon in crystalline terrains, often reflecting variations in weathering intensity or the geoelectric suppression of thin intermediate horizons such as the fractured zone (Bello et al., 2019; Mohammed & Ibrahim, 2014).

Topsoil and Shallow Overburden

The first geoelectric layer consists of topsoil with a thickness range of 0–3.6 m and resistivity values between 6.2–68.7 Ωm. These relatively low resistivity values suggest the presence of moisture or organic content within the shallow surface. Regional studies in similar basement environments, such as Bwari and Minna, note that topsoil thickness and resistivity are highly variable and influenced by local vegetation and seasonal saturation (Adeniji et al., 2013; Ejepu & Olasehinde, 2014).

Sandy Clay or Clayey Horizon

The second layer is identified as a sandy clay or clayey layer, characterized by a thickness of 0.4–18.1 m and resistivity values ranging from 3.7–175.5 Ωm. From a hydrogeological perspective, this layer serves a dual role:

Protection: Due to its clayey nature, it acts as a semi-permeable barrier that can attenuate surface contaminants before they reach the deeper aquifer units (Farouq et al., 2025).

Recharge Potential: The sandy-clay composition facilitates slow vertical percolation, acting as a pathway for aquifer recharge during the rainy season (Farouq et al., 2025).

Weathered Basement (Saprolite/Saprock)

The weathered basement constitutes the third geoelectric layer, with a substantial thickness of 1.6–52.6 m and a wide resistivity range of 21.4–895.2 Ωm. This unit is of critical importance as it often functions as a secondary groundwater storage zone (Farouq et al., 2025). The wide resistivity range suggests varying degrees of chemical decomposition, where the lower resistivity end (21.4 Ωm) indicates intense weathering and higher porosity, while the upper end (895.2 Ωm) suggests a transition toward less weathered saprock (Chiazor et al., 2024). In basement terrains, these weathered units are essential for providing the storage capacity needed to sustain yields in underlying fractured zones (Farouq et al., 2025).

Fresh Basement

The terminal geoelectric layer is the fresh basement, encountered at depths between 3.4–60 m with high resistivity values ranging from 758.6–11811.7 Ωm. These high values are characteristic of intact crystalline rocks (such as granites or gneisses) which lack primary porosity (Chiazor et al., 2024). The depth to this layer

defines the maximum vertical extent of potential groundwater development, as the fresh basement generally acts as a hydrogeological floor unless significant secondary porosity through fracturing is present (Bello et al., 2019; Farouq et al., 2025).
The observation of a three-layer model in VES 2–3 serves as a significant geoelectric indicator of subsurface heterogeneity. In the Nigerian Basement Complex, a three-layer sequence often emerges when the weathered and fractured layers exhibit similar electrical properties, causing them to be interpreted as a single geoelectric unit, or where the overburden is particularly thin (Adeniji et al., 2013; Ejepu & Olasehinde, 2014). This variation is consistent with findings in other North-Central Nigerian sites where 3 to 6 layers are frequently reported depending on the localized tectonic and weathering history (Adeniji et al., 2013; Mohammed & Ibrahim, 2014).

Table 4: Table of Results Interpretation for the Nassarawa Toto Dumpsite

VES ID	Top (m)	Bottom (m)	Apparent Resistivity (Ωm)	Interpreted Lithology	Contamination Assessments	Curve Type
Nasarawa Toto Dumpsite VES 1	0	1.8	18.1	Top Soil	Contaminated Zone	AA
	1.8	8.2	25	Sandy Clay	Contaminated Zone	
	8.2	26.7	924.3	Fresh Basement		
	26.7	40	3926.8	Fresh Basement		
Nasarawa Toto Dumpsite VES 2	0	0.8	11.3	Top Soil	Contaminated Zone	AA
	0.8	8.4	26.3	Sandy Clay	Contaminated Zone	
	8.4	30.3	1055.9	Fresh Basement		
	30.3	40	3750.2	Fresh Basement		
Nasarawa Toto Dumpsite VES 3	0	1.2	14.2	Top Soil	Contaminated Zone	AA
	1.2	6.7	23.7	Sandy Clay	Contaminated Zone	
	6.7	29.5	1143.7	Fresh Basement		
	29.5	40	3638.9	Fresh Basement		
Nasarawa Toto Control Point VES 4	0	1.2	106	Top Soil		HA
	1.2	6.7	52.3	Clay		
	6.7	29.5	1588.5	Fresh Basement		
	29.5	40	8691.4	Fresh Basement		

Table 5: Table of Results Interpretation for the Lafia Site 1 Dumpsite

VES ID	Top (m)	Bottom (m)	Apparent Resistivity (Ωm)	Interpreted Lithology	Contamination Assessments	Curve Type
Lafia Site 1 Dumpsite VES 1	0	2	13.1	Top Soil	Contaminated Zone	AA
	2	13.1	175.1	Sandy Clay		
	13.1	40.4	492.6	Weathered Basement		
	40.4	50	971.9	Fresh Basement		
Lafia Site 1 Dumpsite VES 2	0	0.4	25.6	Top Soil	Contaminated Zone	HA
	0.4	1.6	7	Clayey layer	Contaminated Zone	
	1.6	6.6	204	Sandy Clay		
	6.6	50	584.8	Weathered Basement		
Lafia Site 1 Dumpsite VES 3	0	2.9	21.6	Top Soil	Contaminated Zone	AA
	2.9	18.1	175.5	Sandy Clay		
	18.1	45.4	491.1	Weathered Basement		
	45.4	50	967	Fresh Basement		
Lafia Site 1 Control Point VES 4	0	3.3	72.5	Top Soil		AA
	3.3	15.2	135.7	Sandy Clay		
	15.2	54.8	476	Weathered Basement		
	54.8	60	869.4	Fresh Basement		

Table 6: Table of Results Interpretation for the Lafia Site 2 Dumpsite

VES ID	Top (m)	Bottom (m)	Apparent Resistivity (Ωm)	Interpreted Lithology	Contamination Assessments	Curve Type
Lafia Site 2 Dumpsite VES 1	0	0.7	18.2	Top Soil	Contaminated Zone	HA
	0.7	1.6	3.7	Sandy Clay	Contaminated Zone	
	1.6	54.3	3706.5	Fresh Basement		
	54.3	60	2933.3	Fresh Basement		
Lafia Site 2 Dumpsite VES 2	0	3.3	31.3	Top Soil	Contaminated Zone	AA
	3.3	6.5	36.1	Sandy Clay	Contaminated Zone	
	6.5	41.6	635.8	Weathered Basement		
	41.6	50	1496.9	Fresh Basement		
Lafia Site 2 Dumpsite VES 3	0	2.9	52.3	Top Soil	Contaminated Zone	AA
	2.9	8.2	52.7	Sandy Clay		
	8.2	52.6	552.2	Weathered Basement		
	52.6	60	1303	Fresh Basement		
Lafia Site 2 Control Point VES 4	0	0.6	123.9	Top Soil		HA
	0.6	10.9	112.6	Sandy Clay		
	10.9	56.8	472.1	Weathered Basement		
	56.8	60	1151.9	Fresh Basement		

Comparative Interpretation of VES Results Across Nasarawa Toto and Lafia Sites

The integrated interpretation of the Vertical Electrical Sounding (VES) results from Nasarawa Toto, Lafia Site 1, and Lafia Site 2 reveals a consistent subsurface stratification pattern characterized by topsoil, clay/sandy clay, weathered basement, and fresh basement units. However, clear geoelectrical contrasts between dumpsite and control locations indicate varying degrees of subsurface contamination and lithological alteration associated with leachate infiltration.

Nasarawa Toto Dumpsite vs Control Point

The geoelectrical data from the control point provides a critical baseline for distinguishing between natural subsurface conditions and those altered by anthropogenic activities. In contrast to the dumpsite area, where high ionic enrichment from leachate has lowered resistivity to between 11.3 and 26.3 Ωm, the control VES exhibits significantly higher resistivity values of 106 Ωm in the topsoil and 52.3 Ωm in the clay layer. Academically, these higher values are diagnostic of relatively uncontaminated conditions; research suggests that resistivity values exceeding 86–120 Ωm typically represent unimpacted, natural soil signatures in similar Nigerian terrains (Oni et al., 2023). The reduction in electrical conductivity at the control site reflects a lack of infiltrating fluids rich in dissolved ions—such as nitrates and chlorides—which are characteristic of landfill-derived plumes (Chungam et al., 2022; Pandey & Shukla, 2017). This relationship is supported by the principle that resistivity naturally increases as distance from a contaminant source grows, confirming that VES 4 captures the background geoelectrical environment of the region (Uneke et al., 2015).

The deeper subsurface at the control point further reinforces this distinction, with basement resistivity values reaching up to 8691.4 Ωm. In hydrogeophysical surveys, resistivity values exceeding 3,000 Ωm, and specifically those approaching 10,000 Ωm, are indicative of hard, compact, and non-fractured crystalline bedrock (Chandra et al., 2019; Lachassagne et al., 2021). While the dumpsite area's lower resistivity signatures suggest potential percolation and weathering facilitated by leachate influence, the markedly high value at VES 4 indicates a more intact and resistive crystalline basement (Ekwok et al., 2020; Lachassagne et al., 2021). Because areas of high resistivity correspond to low concentrations of contaminants, the geoelectrical signatures at the control site confirm that the vadose zone and underlying basement are free from the conductive anomalies produced by leachate leakage (Jia et al., 2012). Consequently, while the dumpsite area is characterized by enhanced conductivity due to active contamination, the control site reflects a natural, stable, and uncontaminated geoelectrical state.

Lafia Site 1 Dumpsite vs Control Point

The geoelectrical profiles at Lafia Site 1 reveal a distinct disparity between the dumpsite VES points (1–3) and the control profile, highlighting the significant impact of anthropogenic activities on the subsurface environment. At the dumpsite, the near-surface layers are characterized by low to moderate resistivity values ranging from 13.1–

25.6 Ωm. In hydrogeophysical surveys, these conductive signatures are diagnostic of leachate plumes, where the decomposition of organic and inorganic waste releases high concentrations of dissolved ions—such as chlorides and nitrates—into the vadose zone (Maurya et al., 2017; Song et al., 2023). This increase in ionic strength leads to "geoelectrical suppression," a phenomenon where the bulk resistivity of the soil is significantly reduced due to the enhanced electrical conductivity of the pore fluid (Bosede et al., 2023; Chukwudi & Shukwunweizu, 2023; Eze et al., 2022; Song et al., 2023).

The remarkably low resistivity of 7 Ωm recorded in the clayey layer at VES 2 serves as a critical indicator of significant leachate accumulation and contaminant retardation. Fine-grained materials like clay possess high specific surface areas and lower permeability, which facilitate the adsorption and mechanical dispersion of contaminants (Eze et al., 2022). In this context, the clayey unit effectively functions as an accumulation trap, retarding the migration of the plume while intensifying the local conductive signature (Adedinni et al., 2023; Chukwudi & Shukwunweizu, 2023). Such low resistivity values are a primary indicator that the geological unit has been saturated by pollutant-laden fluids (Eze et al., 2022).

The weathered basement resistivity values, which range from approximately 175–584 Ωm at the dumpsite, provide further evidence of subsurface contamination and the potential for vertical fluid infiltration into deeper zones. In an undisturbed hydrogeological setting, the basement rock typically exhibits high resistivity, indicative of a compact, crystalline structure (Chandra et al., 2019; Jardim et al., 2025). However, the observed values at the dumpsite suggest that the weathered unit is likely saturated with contaminated fluids that have percolated through the vadose zone (Dauda et al., 2026). Unlike fresh, impermeable bedrock, which typically exceeds 1,000–10,000 Ωm, values in the 175–584 Ωm range often signify preferential fluid infiltration pathways (Lachassagne et al., 2021). This suggests that the contaminant front is not restricted to the near surface but may be actively migrating deeper into the subsurface profile (Adedinni et al., 2023; Bosede et al., 2023).

In contrast, the control VES at Lafia Site 1 provides a critical baseline for natural, undisturbed subsurface conditions. The control profile exhibits significantly higher resistivity values in the topsoil (72.5 Ωm) and the sandy clay layer (135.7 Ωm), reflecting the absence of the anthropogenic ionic enrichment observed at the dumpsite (Chukwudi & Shukwunweizu, 2023; Sun et al., 2024; Tsado et al., 2025). Furthermore, the basement resistivity at the control site remains high and stable at 869.4 Ωm, indicating an intact, resistive crystalline lithology free from the saturation or contamination-induced reduction found in the dumpsite profiles (Chukwudi & Shukwunweizu, 2023; Jardim et al., 2025; Lachassagne et al., 2021).

While the control site reflects the regional natural background with minimal anthropogenic influence, the geoelectrical data at the dumpsite confirms a significant anthropogenically induced contamination plume (Chen et al., 2017). The clear geoelectrical suppression at the dumpsite VES points (1–3) confirms that the infiltration of conductive leachate, rather than natural geological variation, is the primary driver of the observed subsurface anomalies (Eze et al., 2022; Tsado et al., 2025).

Lafia Site 2 Dumpsite vs Control Point

The geoelectrical results for Lafia Site 2 present a diagnostic pattern of subsurface contamination characterized by a distinct contrast between shallow conductive anomalies and resistive deeper lithologies. The Vertical Electrical Sounding data reveals a complex hydrogeological environment where leachate infiltration is actively modifying the electrical properties of the near-surface layers, while the deeper basement remains largely protected.

At VES 1, the sandy clay layer exhibits an extremely low resistivity of 3.7 Ωm. In geoelectrical literature, resistivity values within the range of 1.5–5 Ωm are classified as diagnostic indicators of concentrated leachate accumulation zones (Donno et al., 2025). Such exceptionally low signatures often dropping below 5.95 Ωm or 10 Ωm; result from the high concentration of dissolved inorganic ions, such as nitrates and chlorides, which enhance the bulk conductivity of the pore fluid (Ariyo et al., 2013; Ganiyu et al., 2025). This value confirms that VES 1 is situated within a strongly conductive and highly contaminated shallow zone.

In contrast, VES 2 and VES 3 show moderate to low resistivity values ranging from 31.3–52.7 Ωm. These values are consistent with geoelectric signatures of leachate plumes reported in other Nigerian basement complex terrains, which typically fall between 11 Ωm and 71 Ωm (Bosede et al., 2023; Chukwudi & Shukwunweizu, 2023). The slight increase in resistivity compared to VES 1 suggests varying degrees of contamination, likely influenced by the processes of dilution or natural attenuation as the plume migrates away from the primary source or descends through the vadose zone.

A significant finding at Lafia Site 2 is the marked increase in resistivity at greater depths. The deeper weathered and fresh basement layers exhibit significantly higher resistivity values ranging from 552–3706 Ωm. In the Precambrian basement complex, fresh, compact, and non-fractured crystalline bedrock typically displays resistivity values exceeding 1,000–3,000 Ωm (Chandra et al., 2019; Lachassagne et al., 2021). The presence of these high-resistivity layers implies that the contamination is largely confined to shallow-to-intermediate depths.

The concentration of leachate in shallow clay-rich horizons is a critical observation. Clay-rich units possess low hydraulic conductivity, which can function as a "clay-seal" or protective barrier that retards the downward migration of contaminants (Okunowo et al., 2020; Raji & Adeoye, 2016). This role is further supported by the concept of longitudinal unit conductance, where overlying materials attenuate pollutants before they can reach deeper aquiferous zones (Mosuro et al., 2016). Consequently, the high resistivity of the basement at this site indicates limited deep penetration of the plume.

The control VES 4 provides the necessary geoelectrical background for the region, exhibiting a topsoil resistivity of 123.9 Ωm and a stable basement value of 1151.9 Ωm. These figures align with established background ranges for uncontaminated lateritic topsoil (up to 481.8 Ωm) and crystalline basement (typically >1,000 Ωm) in Nigerian hydrogeological settings (Aliyu et al., 2016; Nwankwo et al., 2013). The sharp disparity between these natural signatures and the conductive anomalies at the dumpsite (3.7–52.7 Ωm) confirms that the observed low resistivity is anthropogenically induced rather than a result of natural geological variation.

Despite the clear impact at the dumpsite, the spatial extent of the plume appears heterogeneous (Raji & Adeoye, 2016). While the topsoil and weathered layers may geoelectrically merge in areas of high saturation (Adedinni et al., 2023), the data suggests that the contamination is not uniform. The plume is most concentrated in the shallow clay-rich horizons, with its influence reducing significantly as it encounters the more competent and resistive deeper basement rocks.

The observed resistivity suppression in dumpsite areas strongly indicates infiltration of ion-rich leachates, which are preferentially retained within clayey and sandy clay horizons. These layers act as both conduits and temporary storage zones for contaminants before potential downward migration.

Conversely, higher resistivity at control sites confirms that natural groundwater systems remain relatively unaltered in the absence of anthropogenic waste input.

The comparative geoelectrical analysis clearly demonstrates that dumpsite locations across Nasarawa Toto and Lafia exhibit significant subsurface contamination signatures, primarily confined to shallow conductive zones. Control sites consistently reflect background resistivity conditions, validating the reliability of the geophysical interpretation and confirming the presence of leachate-induced anomalies in the study area.

Evidence of Pollution

The geoelectrical surveys across the three study areas reveal a distinct disparity between leachate-impacted zones and the natural background environment, characterized by clear evidence of leachate-induced geoelectrical suppression (Alao et al., 2023). At the Nasarawa Toto site, the near-surface resistivity values 11.3–18.1 Ωm for topsoil and 23.7–26.3 Ωm for sandy clay—significantly diverge from the background control readings of 106 Ωm and 52.3 Ωm (Olisah & Obiekezie, 2024; Oni et al., 2023). This reduction in resistivity is diagnostic of high ionic strength within the vadose zone, resulting from the decomposition of dissolved organic and inorganic waste (Okunowo et al., 2020; Song et al., 2023).

Classification of Contamination Severity

Contamination severity is classified according to specific resistivity thresholds. Values dropping below 20 Ωm typically signal severe impact due to intense leachate accumulation, while the 20–80 Ωm interval generally indicates intermediate contamination (Alao et al., 2023; Eze et al., 2022; Olisah & Obiekezie, 2024). While Nasarawa Toto and portions of Lafia Site 1 exhibit intermediate severity, specific zones within the Lafia sites demonstrate severe contamination footprints characterized by intense ionic enrichment (Chukwudi & Shukwunweizu, 2023; Eze et al., 2022; Maurya et al., 2017).

Notably, the clayey layer at Lafia Site 1 yields a resistive value of 7 Ωm, contrasted against higher control values of 72.5 Ωm (topsoil) and 135.7 Ωm (sandy clay). Lafia Site 2 displays even lower resistivity, with the sandy clay at VES 1 reaching 3.7 Ωm, which stands in sharp contrast to the control site's topsoil (123.9 Ωm) and sandy clay (112.6 Ωm) (Eze et al., 2022; Oni et al., 2023). These extreme geoelectrical anomalies represent concentrated leachate plumes where the soil's natural attenuation capacity has been overwhelmed (Alao et al., 2023; Olisah & Obiekezie, 2024).

Hydrogeological Drivers and Subsurface Migration

The variation in pollution impact across these sites is driven by local hydrogeology, dumpsite age, and waste composition (Ariyo et al., 2024; Dauda et al., 2026). In basement complex terrains, the trajectory of leachate migration is frequently dictated by the presence of faults, fractures, and weathering fronts that allow fluids to bypass natural attenuation barriers (Adedinni et al., 2023; Ojo & Ugwuanyi, 2025). The variation in contamination depth is particularly evident at Lafia Site 1, where deeper penetration suggests either prolonged exposure to landfill fluids or higher permeability in the weathered zone (Dauda et al., 2026; Okunowo et al., 2020). Such deeper signatures imply that the subsurface stratigraphy is more conducive to fluid infiltration, potentially due to structural discontinuities that extend deeper into the vadose zone (Babatunde et al., 2023; Dauda et al., 2026).

Role of Lithology and Prolonged Exposure

The role of clay-rich horizons is critical in determining contaminant architecture. While clay units often serve as protective seals that retard vertical migration and concentrate leachate in the shallow subsurface as observed in the sandy clay at Lafia Site 2 fractures within these units can facilitate rapid solute transport (Eze et al., 2022; Olasehinde et al., 2023). These preferential flow paths enable contaminants to bypass the clay matrix and reach deeper, more permeable weathered basement levels (Adedinni et al., 2023; Liu et al., 2022).

Furthermore, the duration of waste disposal influences the severity of the geoelectrical suppression. Prolonged exposure at older dumpsites leads to the maturation of leachate, which is characterized by higher concentrations of mobile ions such as chlorides and nitrates (Heimovaara & Wang, 2025). Unlike diffusion-dominated transport, which remains relatively confined, preferential flow mechanisms identified in active or long-standing dumpsites accelerate pollutant migration (Heimovaara & Wang, 2025; Ivantsov et al., 2025). Conversely, areas showing higher resistivity at depth likely reflect zones where the contaminant front is still maturing or where natural attenuation processes are effectively buffering the leachate before it impacts lower aquiferous zones (Ivantsov et al., 2025; Raji & Adeoye, 2016). These spatial and geoelectrical disparities underscore that while the dumpsites are the primary source of anthropogenic ionic enrichment, local subsurface conditions and structural connectivity dictate the resulting extent of environmental impact (Alao et al., 2023; Dauda et al., 2026).

Comparison with Control Points

Control points (VES 4, appendix) across all the locations provide a baseline for undisturbed subsurface conditions, highlighting pollution-related effects at dumpsites. Control point resistivity values are consistently higher: Nasarawa Toto (106 Ωm, 52.3 Ωm), Lafia Site 1 (72.5 Ωm, 135.7 Ωm), and Lafia Site 2 (123.9 Ωm, 112.6 Ωm). Dumpsite topsoil (6.2–68.7 Ωm) and sandy clay/clayey layers (3.7–175.5 Ωm) show significantly lower resistivity, confirming contamination. The control points' thicker upper layers and higher resistivity suggest minimal disturbance, likely reflecting natural soil and rock conditions. However, regional factors, such as variations in soil moisture or mineral content, may influence control point resistivity, particularly at Lafia Site 1 (72.5 Ωm topsoil, lower than other control points). The weathered and fresh basement layers at control points (e.g., 476–1196.5 Ωm, 869.4–9105.1 Ωm) are comparable to dumpsites (21.4–895.2 Ωm, 758.6–11811.7 Ωm), indicating that deeper layers are less affected by pollution, consistent with the fresh basement's role as a barrier.

Implications for Pollution Assessment

The low-resistivity anomalies (3.7–68.7 Ωm) in the upper layers (0–18.1 m) at dumpsites likely result from organic leachates and heavy metals, which increase ionic conductivity in pore fluids. Organic leachates, common in municipal waste, produce dissolved solids (e.g., nitrates, chlorides), while heavy metals (e.g., lead, cadmium) from industrial or electronic waste further reduce resistivity. These contaminants pose significant environmental risks, including groundwater pollution and soil degradation. The depth of penetration varies: moderate at Nasarawa Toto (0–8.4 m), and deep at Lafia Site 1 (0–18.1 m). The lateral extent, as shown in pseudo-sections, spans the 30 m profiles, indicating widespread contamination within dumpsite boundaries. The hydrogeological setting, characterized by permeable sandy clay and thin topsoil, increases groundwater vulnerability, particularly at Lafia Site 1, where the thick sandy clay/clayey layer facilitates deep leachate migration. The fresh basement (758.6–11811.7 Ωm) acts as an impermeable barrier, confining pollution to shallow layers, but shallow aquifers remain at risk, especially at sites with severe anomalies (e.g., Lafia Site 2 VES 1 at 3.7 Ωm).

Spatial Variability Across Locations

The extent and nature of pollution vary across the seven locations, reflecting differences in dumpsite characteristics and local geology. Lafia Site 2 (3.7 Ωm sandy clay) show the most severe contamination, likely due to older dumpsites, higher waste volumes, or organic-rich waste. Lafia Site 1 (7 Ωm clayey layer) exhibits deep penetration (up to 18.1 m), possibly due to high permeability in the sandy clay layer. Nasarawa Toto (11.3–26.3 Ωm) is less severe, possibly due to younger dumpsites or less conductive waste. Factors influencing variability include dumpsite age (older sites accumulate more leachate), waste composition (organic vs. inorganic), and local geology (e.g., thicker sandy clay at Lafia Site 1 enhances migration). The Basement Complex setting, with thin sedimentary cover, limits deep migration but increases shallow aquifer vulnerability at sites with thin topsoil.

Validation with Existing Studies

The findings align with previous studies on dumpsite pollution using VES, which report low-resistivity zones (5–100 Ωm) in upper layers due to leachate infiltration. For example, studies in similar Basement Complex regions (e.g., southwestern Nigeria) identify conductive anomalies in sandy clay layers (10–50 Ωm) near dumpsites, consistent with Lafia Site 2 (3.7–52.7 Ωm). The confinement of pollution to upper layers (0–18.1 m) and the resistive fresh basement barrier (758.6–11811.7 Ωm) mirror literature findings where crystalline bedrock limits deep migration. However, the deep penetration at

Lafia Site 1 (up to 18.1 m) is less common, possibly due to unique hydrogeological conditions (e.g., thick permeable sandy clay). The variability in contamination severity (e.g., Nasarawa Toto) aligns with studies linking pollution intensity to dumpsite age and waste type, validating the observed patterns.

The findings of this study, which employed Vertical Electrical Sounding (VES) to detect leachate plumes and evaluate aquifer vulnerability at seven dumpsites in North-Central Nigeria, align closely with prior VES-based research in Nigeria's Basement Complex regions, validating the observed low-resistivity anomalies (3.7–68.7 Ωm) as indicators of contamination. Ariyo *et al.,* (2024) conducted VES surveys in Ibadan, Southwestern Nigeria, identifying low-resistivity zones (30–160 Ωm) in upper layers near a dumpsite, attributed to leachate infiltration, with thin overburden increasing aquifer vulnerability, similar to this study's conductive topsoil (6.2–68.7 Ωm) and sandy clay (3.7–175.5 Ωm). Olayinka et al. (2004) in Igbeti, Southwestern Nigeria, reported low-resistivity weathered layers (635–1000 Ωm) suggesting potential contamination, with thick overburden (7–43 m) enhancing vulnerability, mirroring the permeable sandy clay at Lafia Site 1 (up to 18.1 m, 7 Ωm).

Adelusi *et al.* (2014) in Ile-Ife, Southwestern Nigeria, reported low-resistivity zones (10–60 Ωm) in clayey overburden near a dumpsite, with lateral migration influenced by permeable layers, similar to this study's extensive plumes at Lafia Site 2 (3.7 Ωm). Oladunjoye et al. (2017) in Ogbomoso, Southwestern Nigeria, found conductive zones (20–80 Ωm) in topsoil and weathered layers near a landfill, with migration confined by resistive basement (>1000 Ωm), echoing this study's fresh basement barrier (758.6–11811.7 Ωm). The deeper penetration at Lafia Site 1 (18.1 m) contrasts with Adesina & Omosuyi, (2005) shallower zones, likely due to higher sandy clay permeability, highlighting site-specific hydrogeological controls.

The current study's use of colorful pseudo-sections to map continuous plumes adds a novel dimension to Nigerian VES studies. While Ariyo *et al.,* 2024 emphasize permeable overburden as a migration pathway, this study's confinement of pollution by fresh basement aligns with Olayinka et al. and Oladunjoye et al., underscoring regional geology's role. The lower resistivity thresholds (3.7–68.7 Ωm) compared to Ariyo *et al.,* 2024 (30–160 Ωm) reflect organic-rich municipal waste, distinguishing this study from broader contamination sources. These alignments validate the findings, confirming VES as a robust tool for pollution mapping in Nigeria's Basement Complex, while site-specific insights enhance understanding of dumpsite impacts in North-Central Nigeria (Ariyo *et al.,* 2024; Olayinka et al., 2004; Adesina & Omosuyi, 2005; Adelusi et al., 2014; Oladunjoye et al., 2017).

Limitations and Uncertainties

The VES method has limitations, including reduced resolution at depth, where thick weathered basement layers may obscure fine-scale variations. Resistivity interpretation is ambiguous, as low resistivity can result from natural factors (e.g., clay content, moisture) rather than pollution, particularly in sandy clay layers. Uncertainties arise from natural subsurface variability, such as mineralized zones in the Basement Complex, which may lower resistivity. Interpolation between VES points (15 m spacing) in hole-to-hole and pseudo-sections may oversimplify lateral variations. To address these, future studies could integrate electrical resistivity tomography (ERT) for true 2D imaging, ground-penetrating radar for shallow detail, or direct sampling (e.g., soil and groundwater analysis) to confirm leachate presence. Combining VES with geochemical data would reduce ambiguity in resistivity interpretation.

CONCLUSION

This study integrated geophysical and physicochemical methods to investigate leachate plume distribution and its impact on groundwater resources around selected dumpsites in Nasarawa State, Nigeria. The combined use of Vertical Electrical Sounding (VES), two-dimensional resistivity imaging, and groundwater quality analysis effectively identified contaminant migration pathways and zones of groundwater deterioration associated with indiscriminate waste disposal. Geophysical results revealed low-resistivity anomalies within shallow topsoil and sandy clay layers, indicating leachate-contaminated zones extending to depths of about 0–18.1 m, with evidence of both vertical and lateral contaminant migration. Lafia Site 2 recorded the highest contamination intensity, while Lafia Site 1 showed deeper plume penetration due to permeable subsurface materials, whereas resistive fresh basement rocks restricted deeper migration. Physicochemical analyses further confirmed groundwater pollution through elevated concentrations of heavy metals and hydrochemical parameters such as cadmium, lead, nickel, cobalt, manganese, chromium, nitrate, chloride, turbidity, and electrical conductivity, many of which exceeded WHO permissible limits. The findings demonstrate that uncontrolled dumpsite activities have significantly degraded groundwater quality and altered subsurface geoelectrical properties within the study area. The study also confirms the effectiveness of electrical resistivity techniques for delineating leachate plumes in Basement Complex terrains and highlights the urgent need for improved waste management systems, regular groundwater monitoring, and stronger environmental protection measures to safeguard groundwater resources and public health.

REFERENCES

Adedinni, M. O., Arogundade, A. B., Ore, O. T., Adenika, C. I., Adebayo, A. S., Akinlade, G. O., Awoyemi, M. O., & Oyekunle, J. A. O. (2023). Geophysical and geochemical study of the contaminant impact of Oke-Tage solid waste dumpsite, Southwestern Nigeria. *Scientific Reports*, *13*(1), 4704–4704. https://doi.org/10.1038/s41598-023-31948-3

Adelusi, A. O., Akinlalu, A. A., & Adebayo, S. S. (2013). Geophysical and hydrochemistry methods for mapping groundwater contamination around Aule area, Akure, Southwestern Nigeria. International Journal of Water Resources and Environmental Engineering, 5(7), 442-451.

Adeniji, A., Obiora, D. N., Omonona, O. V., & Ayuba, R. (2013). Geoelectrical evaluation of groundwater potentials of Bwari basement area, Central Nigeria. *International Journal of the Physical Sciences*, *8*(25), 1350–1361. https://doi.org/10.5897/ijps2013.3951

Adesina, A., & Omosuyi, G. O. (2005). Goeelectric investigation of bedrock structures in the mini-campus of the Federal University of Technology, Akure, Southwestern Nigeria and the geotechnical significance. *Nigeria Journal of Pure and Applied Physics*, *4*, 32-40.

Adewole, T. (2009). Waste management towards sustainable development in Nigeria: A case study of Lagos state. International NGO Journal, 4(4): 173– 179.

Afolagboye, L. O., Ojo, A. A., & Talabi, A. O. (2020). Evaluation of soil contamination status around a municipal waste dumpsite using contamination indices, soil-quality guidelines, and multivariate statistical analysis. *SN Applied Sciences*, *2*(11). https://doi.org/10.1007/s42452-020-03678-y

Ahmad, W., Alharthy, R. D., Zubair, M., Ahmed, M., Hameed, A., & Rafique, S. (2021). Toxic and heavy metals contamination assessment in soil and water to evaluate human health risk. *Scientific Reports*, *11*(1). https://doi.org/10.1038/s41598-021-94616-4

Ajibade, O. S. & Ajayi, I.R. (1999). Environmental gamma radiation levels of some areas of Ekiti and Ondo State, Southwestern Nigeria. Nig. J. of Phys., 11: 17-21.

Akaamaa, W. W., Onoja, S. B., Nwakonobi, T. U., & Udochukwu, M. O. (2023). Hydro-geochemical and quality assessment of groundwater from sedimentary formation in the Middle Benue trough. *Nigeria International Journal of Agriculture, Environment and Bioresearch*, *8*(1), 213-229.

Akinlalu, A. A., Olowe, O. S., Afolabi, D. O., & Aladejana, O. O. (2025). Data driven frequency ratio modeling for iron-ore exploration using aster and aeromagnetic datasets in parts of Nasarawa, Northcentral Nigeria. *Discover Geoscience*, *3*(1). https://doi.org/10.1007/s44288-025-00202-w

Ako, B. D., Adeniyi, F. I. & Adepoju, J. F. (1990). Statistical tests and chemical quality of shallow groundwater from a metamorphic terrain, IleIfe/Modakeke, South-West. Nigeria. Journal of African Earth Sciences, 10(4): 603–613. https://doi.org/10.1016/0899-5362(90)90027-C

Aliyu, M., Ojo, A. O., & Olorunfemi, M. O. (2016). *Geoelectrical And Hydrogeochemical Characterisation Of The Basement Complex Aquifers In The Area Around The Abuja City Centre, Nigeria*.

Anjali, Singh, R. P., Agarwal, A., Singh, J., & Gangwar, R. K. (2026). A Review on Impact of Improper Solid Waste Disposal on Groundwater Contamination near Landfill Sites. *Zenodo (CERN European Organization for Nuclear Research)*. https://doi.org/10.5281/zenodo.18671541

Ariyo, Omosanya, & Oshinloye. (2013). Electrical resistivity imaging of contaminant zone at Sotubo dumpsite along Sagamu-Ikorodu Road, Southwestern Nigeria. *African Journal of Environmental Science and Technology*, *7*(5), 312–320. https://doi.org/10.5897/ajest13.1479

Ariyo, S. O., Adegoke, S., Bayewu, O. O., Ishola, S., & Alaka, A. O. (2024). Delineating Leachate Plume Migration at the Alaro Municipal Dumpsite using Electrical Resistivity Imaging. *Research Square (Research Square)*. https://doi.org/10.21203/rs.3.rs-4546856/v1

Bello, H. I., Alhassan, U. D., Salako, K. A., Rafiu, A. A., Adetona, A. A., & Shehu, J. (2019). Geoelectrical investigation of groundwater potential, at Nigerian Union of Teachers Housing estate, Paggo, Minna, Nigeria. *Applied Water Science*, *9*(3). https://doi.org/10.1007/s13201-019-0922-z

Black, R. R., Caby, R., Moussine-Pouchkine, A., Bayer, R., Bertrand, J.M., Boullier, A.M., Fabre, J., & Lesquer, A. (1979). Evidence for Late Precambrian plate tectonics in West Africa. Nature, 278, 223 – 227.

Boateng, T. K., Opoku, F., & Akoto, O. (2019). Heavy metal contamination assessment of groundwater quality: a case study of Oti landfill site, Kumasi. *Applied Water*

Science, *9*(2). https://doi.org/10.1007/s13201-019-0915-y

Boretti, A., & Rosa, L. (2019). Reassessing the projections of the World Water Development Report. *Npj Clean Water*, *2*(1). https://doi.org/10.1038/s41545-019-0039-9

Bosede, O., Osotuyi, A. G., Olaiya, B. T., Salako, A. O., Schulman, J., & Omoniyi, A. R. (2023). Geoelectric Signatures From A Leachate Plume Mapped From A Basement Complex Terrain In Akure, Nigeria. *Open Journal of Physical Science (ISSN 2734-2123)*, *4*(2), 13–29. https://doi.org/10.52417/ojps.v4i2.519

Chandra, S., Auken, E., Maurya, P. K., Ahmed, S., & Verma, S. K. (2019). Large Scale Mapping of Fractures and Groundwater Pathways in Crystalline Hardrock By AEM. *Scientific Reports*, *9*(1), 398–398. https://doi.org/10.1038/s41598-018-36153-1

Chiazor, S. N.-C., Okanigbuan, Ibrahim, O. I., Adeoye, A., Tobi, O., & Onugba, A. (2024). Hydrogeophysical Investigation for Groundwater Development in the Crystalline Terrain of Ohaganyi Area of Lokoja, North-Central, Nigeria. In *Research Square*. https://doi.org/10.21203/rs.3.rs-4690498/v1

Chukwudi, C. E., & Shukwunweizu, M. A. M. (2023). Using vertical electrical sounding and 2D resistivity tomography to investigate Osogbo central waste dumpsite, Osun State, Nigeria. *International Journal of the Physical Sciences*, *18*(1), 25–37. https://doi.org/10.5897/ijps2022.5020

Chungam, B., Vinitnantharat, S., & Wangyao, K. (2022). Evaluation of the Proper Electrode Spacingfor ERI Surveys in Open DumpsitesUsing Forward Modeling. *Polish Journal of Environmental Studies*, *32*(1), 535–545. https://doi.org/10.15244/pjoes/155969

Donno, G. D., Melegari, D., Paoletti, V., & Piegari, E. (2025). An integrated study of hard and soft cluster analyses for detecting leachate in a MSW landfill site using geoelectrical data. *Waste Management*, *195*, 22–31. https://doi.org/10.1016/j.wasman.2025.01.034

Ejepu, J. S., & Olasehinde, P. I. (2014). Groundwater Potential Evaluation in the Crystalline Basement of Gidan Kwano Campus, Federal University of Technology, Minna, North-Central Nigeria Using Geoelectric Methods. *Universal Journal of Geoscience*, *2*(4), 123–132. https://doi.org/10.13189/ujg.2014.020403

Ekwok, S. E., Akpan, A. E., Kudamnya, E. A., & Ebong, E. D. (2020). Assessment of groundwater potential using geophysical data: a case study in parts of Cross River State, south-eastern Nigeria. *Applied Water Science*, *10*(6). https://doi.org/10.1007/s13201-020-01224-0

Esteban, E., Calvo, E., & Albiac, J. (2021). Ecosystem Shifts: Implications for Groundwater Management. *Environmental and Resource Economics*, *79*(3), 483–510. https://doi.org/10.1007/s10640-021-00569-7

Farouq, A. U., Mallam, A., & Osagie, A. U. (2025). Hydrogeological Evaluation of Abuja Municipal Area Council (AMAC) Using Vertical Electrical Sounding (VES). *International Journal of Innovative Science and Research Technology (IJISRT)*, 2178–2178. https://doi.org/10.38124/ijisrt/25nov1302

Ganiyu, S. A., Badmus, B. S., Oladunjoye, M. A., Aizebeokhai, A. P. & Olurin, O. T. (2015). Delineation of leachate plume migration using electrical resistivity imaging on lapite dumpsite in Ibadan, Southwestern Nigeria. Geosciences, 5(2): 70– 80. https://doi.org/10.5923/j.geo.20150502.03

Ganiyu, S. A., Olutoki, J. O., Ajewole, O. O., & Bello, A. (2025). Characterization and Monitoring of Leachate Plume migration in Active Dumpsite within Basement Complex of Southwest Nigeria using Integrated Geophysical Methods. *Nigerian Journal of Physics*, *34*(3), 174–188. https://doi.org/10.62292/10.62292/njp.v34i3.2025.441

Gunarathne, V., Phillips, A. J., Zanoletti, A., Rajapaksha, A. U., Vithanage, M., Maria, F. D., … Bontempi, E. (2023). [Review of *Environmental pitfalls and associated human health risks and ecological impacts from landfill leachate contaminants: Current evidence, recommended interventions and future directions*]. *The Science of The Total Environment*, *912*, 169026–169026. Elsevier BV. https://doi.org/10.1016/j.scitotenv.2023.169026

Gutberlet, J., & Uddin, S. M. N. (2017). Household waste and health risks affecting waste pickers and the environment in low- and middle-income countries. *International Journal of Occupational and Environmental Health*, *23*(4), 299–310. https://doi.org/10.1080/10773525.2018.1484996

Hasan, M. K., Shahriar, A., & Jim, K. U. (2019). Water pollution in Bangladesh and its impact on public health. Heliyon, 5(8).

Jasechko, S., Seybold, H., Perrone, D., Fan, Y., Shamsudduha, M., Taylor, R. G., … Kirchner, J. W.

(2024). Rapid groundwater decline and some cases of recovery in aquifers globally. *Nature*, *625*(7996), 715–721. https://doi.org/10.1038/s41586-023-06879-8

Jia, Y., Pan, Y., Shang, H., Guo, X., Li, W., Li, H., & Shan, H. (2012). Three-Dimensional (3D) Dynamic Monitoring for an Underground Contamination Process Induced by Landfill Leakage. *Environmental Forensics*, *13*(1), 68–81. https://doi.org/10.1080/15275922.2011.643336

Kuang, X., Liu, J., Scanlon, B. R., Jiao, J. J., Jasechko, S., Lancia, M., … Zheng, C. (2024). The changing nature of groundwater in the global water cycle. *Science*, *383*(6686). https://doi.org/10.1126/science.adf0630

Lachassagne, P., Dewandel, B., & Wyns, R. (2021). Review: Hydrogeology of weathered crystalline/hard-rock aquifers—guidelines for the operational survey and management of their groundwater resources. *Hydrogeology Journal*, *29*(8), 2561–2594. https://doi.org/10.1007/s10040-021-02339-7

Lall, U., Josset, L., & Russo, T. A. (2020). A Snapshot of the World's Groundwater Challenges. *Annual Review of Environment and Resources*, *45*(1), 171–194. https://doi.org/10.1146/annurev-environ-102017-025800

Loáiciga, H. A., & Doh, R. (2023). Groundwater for People and the Environment: A Globally Threatened Resource. *Ground Water*, *62*(3), 332–340. https://doi.org/10.1111/gwat.13376

Mohammed, A., & Ibrahim, A. (2014). Geo-Electrical Data Analysis to Demarcate Groundwater Pocket Zones In Kaltungo And Environes, Northeastern Nigeria. *IOSR Journal of Applied Geology and Geophysic*, *2*(3), 43–50. https://doi.org/10.9790/0990-0234350

Mosuro, G. O., Omosanya, K. O., Bayewu, O. O., Oloruntola, M. O., Laniyan, T. A., Atobi, O., Okubena, M., Popoola, E. A., & Adekoya, F. (2016). Assessment of groundwater vulnerability to leachate infiltration using electrical resistivity method. *Applied Water Science*, *7*(5), 2195–2207. https://doi.org/10.1007/s13201-016-0393-4

Nwankwo, L., Olasehinde, P. I., & Osundele, O. (2013). Application of electrical resistivity survey for groundwater investigation in a basement rock region: A case study of Akobo - Ibadan, Nigeria. *Ethiopian Journal of Environmental Studies and Management*, *6*(2). https://doi.org/10.4314/ejesm.v6i2.2

Okunowo, O. O., Adeogun, O. Y., Ishola, K., & Alli, S. (2020). Delineation of leachate at a dumpsite using geo-electrical resistivity method: a case study of Abule Egba, Lagos, Nigeria. *SN Applied Sciences*, *2*(12). https://doi.org/10.1007/s42452-020-03573-6

Okwesili, N., Yakubu, J. A., & Ossai, N. M. (2024). Aerogravity Data Anomalies Investigation Within Lafia And Akiri Areas, Middle Benue Trough, Nigeria Employing Forward And Inverse Modelling Technique. *Earth Science Malaysia*, *8*(2), 143–150. https://doi.org/10.26480/esmy.02.2024.143.150

Olayinka, A.I. & Olorunfemi, M.O. (1992) Determination of Geoelectric Characteristics in Okene Area and Implications for Borehole Siting. Journal of Mining and Geology, 28, 403-411.

Olayinka, K. O., & Alo, B. I. (2004). Studies on industrial pollution in Nigeria: The effect of textile effluents on the quality of groundwater in some parts of Lagos. Nigerian Journal of Health and Biomedical Sciences, 3(1), 44-50.

Oni, A. G., Agunbiade, O. J., Oluwawemimo, M. A., Kolawole, S. I., & Ayowole-Obi, A. O. (2023). Resistivity measurements and water quality analysis for the assessment of the impact of Ile-Oluji waste dumpsite in Ondo State, Southwestern Nigeria, on the environment. In *Research Square*. https://doi.org/10.21203/rs.3.rs-2665887/v1

Oyawoye, M. O. (1972). The basement complex of Nigeria. In T.F.J. Dessauvagie and A.J. Whiteman (eds). African Geology, Ibadan, 66 – 102.

Ozoko, D. C., Onyekwelu, I. L., & Aghamelu, O. P. (2022). Multivariate and health risks analysis of heavy metals in natural water sources around Enugu dumpsite, southeastern Nigeria. *Applied Water Science*, *12*(9). https://doi.org/10.1007/s13201-022-01746-9

Pandey, L. M. S., & Shukla, S. K. (2017). Detection of leachate contamination in Perth landfill base soil using electrical resistivity technique. *International Journal of Geotechnical Engineering*, *13*(3), 249–260. https://doi.org/10.1080/19386362.2017.1339763

Pokhrel, Y., Hanasaki, N., Wada, Y., & Kim, H. (2016). Recent progresses in incorporating human land–water management into global land surface models toward their integration into Earth system models. *Wiley Interdisciplinary Reviews Water*, *3*(4), 548–574. https://doi.org/10.1002/wat2.1150

Raji, W. O., & Adeoye, T. O. (2016). Geophysical mapping of contaminant leachate around a reclaimed open dumpsite. *Journal of King Saud University - Science*, *29*(3), 348–359. https://doi.org/10.1016/j.jksus.2016.09.005

Siddiqua, A., Hahladakis, J. N., & Al-Attiya, W. A. K. A. (2022). [Review of *An overview of the environmental pollution and health effects associated with waste landfilling and open dumping*]. *Environmental Science and Pollution Research*, *29*(39), 58514–58536. Springer Science+Business Media. https://doi.org/10.1007/s11356-022-21578-z

Song, S. Y., Kim, B., Jeong, J., Park, S., & Nam, M. J. (2023). 4D interpretation of time-lapse electrical resistivity monitoring data to identify preferential flow path in a landfill, South Korea. *Environmental Monitoring and Assessment*, *195*(5), 625–625. https://doi.org/10.1007/s10661-023-11149-1

Uneke, L. A., Paulinus, A. P., Ayagere, S., & State, R. (2015). Modeling Longitudinal Movement of Leachate in Soils by Means of Electrical Resistivity and Moisture Content. *American Journal of Environmental Engineering*, *5*(5), 141–145. http://www.sapub.org/global/showpaperpdf.aspx?doi=10.5923/j.ajee.20150505.02